[Papers in Palaeontology, 2020, pp. 1–27]

REDESCRIPTION AND PHYLOGENETIC AFFINITIES OF THE CAIMANINE *EOCAIMAN CAVERNENSIS* (CROCODYLIA, ALLIGATOROIDEA) FROM THE EOCENE OF ARGENTINA

by PEDRO L. GODOY[1], GIOVANNE M. CIDADE[2,3], FELIPE C. MONTEFELTRO[4], MAX C. LANGER[2] *and* MARK A. NORELL[5]

[1]Department of Anatomical Sciences, Stony Brook University, Stony Brook, NY USA; pedrolorenagodoy@gmail.com
[2]Laboratório de Paleontologia de Ribeirão Preto, FFCLRP, Universidade de São Paulo, Ribeirão Preto, Brazil; giovannecidade@hotmail.com, mclanger@ffclrp.usp.br
[3]Laboratório de Estudos Paleobiológicos, Departamento de Biologia, Universidade Federal de São Carlos, Sorocaba, Brazil
[4]Departamento de Biologia e Zootecnia, Universidade Estadual Paulista, FEIS, Ilha Solteira, Brazil; fc.montefeltro@unesp.br
[5]Division of Paleontology, American Museum of Natural History, New York, NY USA; norell@amnh.org

Typescript received 24 April 2020; accepted in revised form 31 July 2020

Abstract: Caimaninae is one of the few crocodylian lineages that still has living representatives. Today, most of its six extant species are restricted to South and Central America. However, recent discoveries have revealed a more complex evolutionary history, with a fossil record richer than previously thought and a possible North American origin. Among the oldest caimanines is *Eocaiman cavernensis*, from the Eocene of Patagonia, Argentina. It was described by George G. Simpson in the 1930s, representing the first caimanine reported for the Palaeogene. Since then, *E. cavernensis* has been ubiquitous in phylogenetic studies on the group, but a more detailed morphological description and revision of the taxon were lacking. Here, we present a reassessment of *E. cavernensis*, based on first-hand examination and micro-computed tomography of the holotype, and reinterpret different aspects of its morphology. We explore the phylogenetic affinities of *E. cavernensis* and other caimanines using parsimony and Bayesian inference approaches. Our results provide evidence for a monophyletic *Eocaiman* genus within Caimaninae, even though some highly incomplete taxa (including the congeneric *Eocaiman itaboraiensis*) represent significant sources of phylogenetic instability. We also found *Culebrasuchus mesoamericanus* as sister to all other caimanines and the North American globidontans (i.e. *Brachychampsa* and closer relatives) outside Caimaninae. A time-calibrated tree, obtained using a fossilized birth–death model, shows a possible Campanian origin for the group (76.97 ± 6.7 Ma), which is older than the age estimated using molecular data, and suggests that the earliest cladogenetic events of caimanines took place rapidly and across the K–Pg boundary.

Key words: Caimaninae, morphology, CT scan, evolution, Bayesian inference, fossilized birth–death model.

At present, six extant species of Caimaninae are distributed within the genera *Caiman*, *Melanosuchus* and *Paleosuchus*. These are found mostly in South and Central America (the only exception is *Caiman crocodilus*, the distribution of which extends as far north as southern Mexico; Thorbjarnarson 1992; Brochu 1999, Grigg & Kirshner 2015). Phylogenetically, Caimaninae is defined as the group that includes *C. crocodilus* and all crocodylians closer to it than to *Alligator mississippiensis* (Brochu 1999, 2003). It belongs to Alligatoroidea, one of the three main lineages of the crown-group Crocodylia, together with Crocodyloidea and Gavialoidea (Brochu 1999, 2003). Within Alligatoroidea, the sister group of Caimanine is Alligatorinae, which is currently represented by only two extant species: *A. mississippiensis* of North America and *A. sinensis* from China (Grigg & Kirshner 2015). Nevertheless, compared with Caimaninae, the fossil record of Alligatorinae has been historically regarded as much richer (Brochu 2010), with a more widespread geographic distribution and several species documented for the Cenozoic (Brochu 1999, 2003; Whiting *et al.* 2016).

In the twenty-first century, however, new discoveries have revealed a higher diversity of Caimanine during the Cenozoic, especially in South America, but also with

doi: 10.1002/spp2.1339

important findings from Central and North America (Aguilera *et al.* 2006; Bona 2007; Brochu 2010; Fortier & Rincón 2013; Hastings *et al.* 2013; Pinheiro *et al.* 2013; Scheyer *et al.* 2013, 2019; Salas-Gismondi *et al.* 2015; Cidade *et al.* 2017; Bona *et al.* 2018; Souza-Filho *et al.* 2019). These new studies and findings added complexity to both the phylogenetic and the biogeographical histories of caimanines. For instance, the discovery of a diverse Miocene caimanine fauna from Central America, as well as even more fossils from South America (Hastings *et al.* 2013; Scheyer *et al.* 2013; Salas-Gismondi *et al.* 2015), revealed some species bearing a mosaic of features. Additionally, the presence of North American taxa deeply nested within Caimaninae (Brochu 2010; Cossette & Brochu 2018) has puzzled researchers about the group's biogeographic history.

In this context, *Eocaiman cavernensis* (Fig. 1) has a central role in improving our understanding of caimanine evolution. Described by the prominent palaeontologist George G. Simpson (Simpson 1933*a*) from Eocene rocks of Argentina, this was the first caimanine species reported for the Palaeogene. Most early phylogenetic studies placed *E. cavernensis* as the sister taxon of all other caimanines (Brochu 1999, 2010, 2011). But in the last decade, increased interest in the group was promoted by new fossil discoveries, which led to updated phylogenetic hypotheses for caimanines, with alternative positions for *E. cavernensis* (e.g. not necessarily in a sister taxon relationship with all other caimanines; Hastings *et al.* 2013, 2016; Scheyer *et al.* 2013; Salas-Gismondi *et al.* 2015; Bona *et al.* 2018). Additionally, two other *Eocaiman* species were proposed, *E. palaeocenicus* and *E. itaboraiensis* (Bona 2007; Pinheiro *et al.* 2013), adding complexity to the biogeographical and phylogenetic histories of the genus as well as to Caimaninae.

In this study, we provide a detailed redescription of *E. cavernensis*, based on first-hand examination of the type specimen, as well as on micro-computed tomography (μCT) data. We use the new information to provide a comprehensive morphological comparison with other caimanines and to rescore this taxon into a recent phylogenetic data matrix. Phylogenetic analyses are performed using both maximum parsimony and Bayesian inference, this latter approach applied for the first time in the context of Caimaninae (i.e. using only morphological characters). We also combined the resultant topology of Caimaninae with information on taxon ages to obtain a time-calibrated phylogeny of the group using the fossilized birth–death (FBD) process, in a Bayesian framework. These results are then used for discussing palaeoecological and palaeobiogeographical implications for the group.

HISTORICAL BACKGROUND AND GEOLOGICAL SETTING

The Scarritt Patagonian Expeditions and the discovery of Eocaiman cavernensis

Between 1930 and 1933, two great expeditions to southern Argentina, known as the Scarritt Patagonian Expeditions, were conducted by the American Museum of Natural History (Madden & Scarano 2010). They were led by the eminent palaeontologist George G. Simpson and yielded several Cenozoic vertebrate fossils. Detailed records of this expedition can be found in Simpson's field notebooks (Simpson 1930*a*, *b*) and in his book *Attending marvels: A Patagonian journal* (Simpson 1934*a*), in which he mentions dozens of fossils collected, mainly mammals. One of the most important sites explored during the first expedition (1930–1931) was the Gran Barranca (Fig. 2), in the Chubut Province (Madden & Scarano 2010). This locality provided some fossil reptiles, including the gigantic snake *Madtsoia bai* (Simpson 1933*b*) and the crocodylian *E. cavernensis* (Simpson 1933*a*).

In a short descriptive paper, Simpson (1933*a*) classified *Eocaiman cavernensis* as 'a true crocodilid or alligatorid', closely related to '*Caiman* and *Jacaré*' (both of which are now assigned to the genus *Caiman*). This was subsequently corroborated by several phylogenetic studies, which consistently included *E. cavernensis* within Caimaninae (Brochu 1999, 2010, 2011; Hastings *et al.* 2013, 2016; Scheyer *et al.* 2013; Pinheiro *et al.* 2013; Salas-Gismondi *et al.* 2015; Bona *et al.* 2018). However, even though *E. cavernensis* has been continually present in numerous phylogenetic analyses since Simpson's work (1933*a*), no detailed descriptive work was conducted for the specimen, which lacks a robust assessment of its morphology.

Geology of the Gran Barranca

Simpson used the term '*Notostylops* Beds' to refer to the geological unit that yielded *E. cavernensis*, following the prior designation of Florentino Ameghino (Ameghino 1906; Simpson 1933*a*). In the subsequent years, different names were proposed for the different units of the Gran Barranca (e.g. Simpson 1933*c*; Cifelli 1985), until Spalletti & Mazzoni (1977, 1979) combined all of them into the Gran Barrancan Member, which was proposed as the lowest member of the Sarmiento Formation (Fig. 2). Finally, Ré *et al.* (2010) proposed the name 'Simpson's Y Tuff' for the specific rock layer originally known as *Notostylops*


A
B
C
D
E
F

FIG. 1. Holotype of *Eocaiman cavernensis* (AMNH FARB 3158). A, dorsal view of the skull. B, ventral view of the skull. C, left lateral view of the skull. D, dorsal view of the mandible. E, ventral view of the mandible. F, left lateral view of the mandible. Scale bar represents 2 cm. Photographs by Mick Ellison.

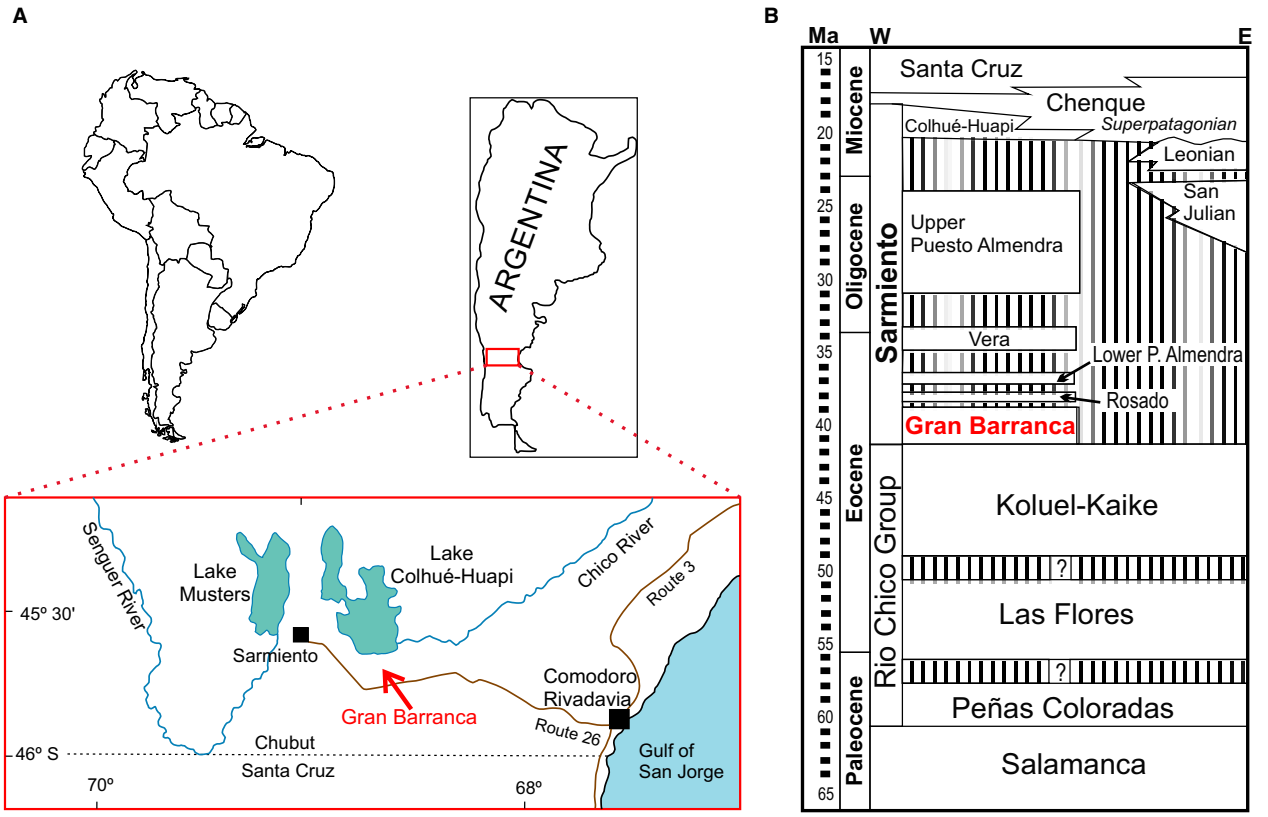

FIG. 2. A, maps depicting the location of the Gran Barranca site (red arrow) in South America and Argentina, where the fossil remains of *Eocaiman cavernensis* were collected during the first Scarritt Patagonian Expedition (1930–1931), led by George G. Simpson. B, schematic stratigraphy of the Cenozoic of central Patagonia, illustrating the middle Eocene age of the Gran Barrancan Member of the Salamanca Formation. Modified from Bellosi (2010).

Beds, but still included it as part of the Gran Barrancan Member.

The precise age of these rocks has been controversial. Simpson (1933*a*) first suggested an Eocene age for the *Notostylops* Beds. Nevertheless, without a precise date for the entire mammalian fauna (which represents most of the fossils found in these rocks), it has been referred to the Casamayoran South American Land Mammal Age (SALMA), one of three SALMAs recognized in the Eocene of South America (Kay *et al.* 1999). Cifelli (1985) then divided the so-called Casamayoran age into two Eocene subages, Barrancan and Vacan, including the *Notostylops* Beds in the former (which is older than the Vacan). More recently, Ré *et al.* (2010) used physical stratigraphy, $^{40}Ar/^{39}Ar$ dating analysis, and magnetic polarity stratigraphy to date the Gran Barrancan Member. They proposed that the Barrancan age would range from 41.6 to 39.0 Ma, which corresponds to a Lutetian–Bartonian (middle Eocene) age according to the International Commission on Stratigraphy (Cohen *et al.* 2013; v2020/01). A Bartonian age was specifically obtained for the Simpson's Y Tuff (= *Notostylops* Beds), with a mean age of 39.85 Ma estimated for its rocks.

MATERIAL AND METHOD

The genus Eocaiman

The presence of *E. cavernensis* in nearly all morphology-based phylogenetic studies of Caimaninae illustrates its

historical and phylogenetic significance. It represents the type species of the genus *Eocaiman* and was described by Simpson (1933*a*) based on a single specimen (AMNH FARB 3158), consisting of a partial skull and almost complete lower jaws (Fig. 1). More recently, two other species were described for the genus. Bona (2007) erected *E. palaeocenicus* based on 13 specimens (MPEF-PV 1933 (holotype), 1935, 1936, MLP 90-II-12-117, 90-II-12-124, 93-XII-10-11, 93-XII-10-13, 95-XII-10-20, 95-XII-10-27, MACN-PV CH 1914, 1915, 1916 and 1627) from the Salamanca Formation (early Paleocene) of Argentina, all of which correspond to mandibular elements or teeth (see also Gasparini 1981, 1996). A third species, *E. itaboraiensis*, was proposed by Pinheiro *et al.* (2013) based on four specimens (three partial left dentaries and one tooth; MCT 1791-R (holotype); MCT 1792-R; MCT 1793-R; MCT 1794-R), from the Itaboraí Basin (late Paleocene) of Brazil. Therefore, *E. cavernensis* is stratigraphically the most recent of the three *Eocaiman* species, as well as the only one with associated cranial material.

In addition, other specimens have tentatively been referred to the genus *Eocaiman*. Langston (1965) referred to *Eocaiman* sp. two fragmentary dentaries (UCPM 38878 and UCPM 39023) from the middle Miocene Honda Group, in La Venta, Colombia (Flynn & Swisher 1995). Although the referral of these dentaries to the genus is nearly consensual, further assessment is required to assign them to any of the three species or to a new taxon (Pinheiro *et al.* 2013). Additionally, an Argentinian specimen housed at the American Museum of Natural History (AMNH FARB 19170) has also been assigned to *Eocaiman*. The specimen is a partial skull (missing most of its rostral and caudal portions), and associated vertebral fragments. According to the museum catalogue card, the material was collected by J. L. Minoprio, in rocks of the 'Divisadero Largo Formation' (possibly middle Eocene; Cerdeño *et al.* 2008; Lopez 2010), west of the city of Mendoza. However, even though previous studies have considered this specimen as belonging to *E. cavernensis*, even to the extent of scoring discrete characters based on it (Brochu 1999, Fortier & Rincón 2013; Pinheiro *et al.* 2013; Fortier *et al.* 2014), further and more detailed investigation is still necessary to confirm its affinities to the species or the genus. For this reason, we did not assume AMNH FARB 19170 as referable to *E. cavernensis*, and therefore did not consider this specimen in the present morphological redescription.

Micro-computed tomography

The type specimen of *E. cavernensis* (AMNH FARB 3158) was μCT scanned at the Microscopy and Imaging Facility of the AMNH, using a GE phoenix v|tome|x s240 scanner (Godoy *et al.* 2020). The scan resulted in 3515 slices, with a resolution of 1000 pixels, voxel size of 0.05517678 mm, magnification ratio of 3.62471325, voltage of 180 kV, and current of 200 μA. Initial visualization of slices, as well as virtual 3D reconstruction and rendering were performed using Volume Graphics VGStudio Max version 2.2, available at the Microscopy and Imaging Facility (AMNH). Segmentation of bones and selected structures was achieved with VGStudio Max version 3.0, available at the vertebrate palaeontology laboratory of Dr Alan Turner, at Stony Brook University.

Phylogenetic analysis

The morphological data matrix used for the phylogenetic analysis performed herein is a modified version of the dataset presented by Cidade *et al.* (2020*a*), which is the most recent of a series of data matrices originating from the work of Brochu (1999, 2011). In terms of taxon sampling, we included *Protocaiman peligrensis* and excluded UCMP 39978 from the matrix of Cidade *et al.* (2020*a*). The scorings of *Protocaiman peligrensis*, a putative caimanine from the Paleocene of Argentina, follow the morphological description in Bona *et al.* (2018). The exclusion of UCMP 39978, a specimen attributed to *Caiman* cf. *lutescens* by Langston (1965), was based on the taxonomic revision of *Caiman lutescens* presented by Bona *et al.* (2012), which assigned this specimen to *Caiman latirostris*.

The scorings of *E. cavernensis* were based solely on the type specimen (AMNH FARB 3158) and did not consider the specimens from the Miocene of Colombia (UCPM 38878 and UCPM 39023) or the one from Mendoza, Argentina (AMNH FARB 19170). Apart from the scorings of *E. cavernensis*, which were thoroughly reassessed here, we also rescored two characters for *Purussaurus brasiliensis*, and one character each for *Eocaiman palaeocenicus*, *Globidentosuchus brachyrostris*, and *Bottosaurus harlani* (for details about rescorings and justifications, see Godoy *et al.* 2020, supporting information). The final matrix was constructed using Mesquite version 3.51 (Maddison & Maddison 2018) and is available in Godoy *et al.* (2020). It contains the same 187 unordered and non-additive characters of the dataset of Cidade *et al.* (2020*a*) and includes 94 eusuchian taxa (88 crocodylians and 6 non-crocodylian eusuchians, with *Bernissartia fagesii* as the operational outgroup for all phylogenetic analyses).

Phylogenetic analysis was performed with equally weighted parsimony, using TNT version 1.5 (Goloboff *et al.* 2008; Goloboff & Catalano 2016). A heuristic tree ('traditional') unconstrained search was conducted performing 20 000 replicates of Wagner trees (using random addition sequences, RAS) with random seed value set to 0, followed by tree bisection and reconnection

(TBR) branch swapping and 10 trees saved per replication. Another round of TBR branch swapping was performed on the best trees obtained at the end of the replicates (saved in memory) and trees were collapsed after the searches. Node retention in most parsimonious trees (MPTs) was measured by calculating Bremer supports (Farris *et al.* 1982; Bremer 1988, 1994). Absolute Bremer support values were obtained using 10 searches of 200 replications each, using TBR branch swapping and retaining up to 20 trees during each replication (commands: hold 10 000; subopt N; mult = tbr replications 200 hold 20; bb = fill). After each run, trees were exported as .ctf files, and TNT memory was erased (command: keep 0). After 10 runs, the total 100 000 trees were imported to TNT and used to calculate absolute Bremer support values (commands: shortread trees.ctf; bsupport).

Furthermore, we also applied the iterative PCR (IterPCR) protocol (Pol & Escapa 2009) for identifying potentially unstable taxa. Within the context that problematic taxa (usually highly fragmented ones) can generate numerous MPTs and a poorly resolved strict consensus, Pol & Escapa (2009) developed this protocol for automatically detecting unstable taxa, avoiding a priori exclusions. This method measures the relative stability of direct descendants of polytomies within the strict consensus, obtaining the PCR measure (reduced positional congruence; Estabrook 1992; Pol & Escapa 2009). We initially applied the faster version of this protocol, using the TNT implementation established by Goloboff & Szumik (2015; command: pcrprune). However, in order to obtain a better visual representation of the alternative positions of unstable taxa, we also used the script designed for the GUI version of TNT. We followed the recommendations in Pol & Escapa (2009), which are specific for when the TNT GUI script is used with more than 100 000 MPTs, and used only a set of randomly sampled trees for diminishing computational time (e.g. for sampling 2000 trees, commands were: tgroup = 0*2000; followed by tchoose {0}). After that, we selected some of the most unstable taxa within the scope of Caimaninae phylogeny and removed those from the final matrix. Then, additional heuristic tree searches were performed, without those unstable taxa, but using the same search parameters as the original search. Bremer support values were also calculated for the MPTs of these additional analyses.

As sensitivity analyses, we also used Bayesian inference to estimate the phylogeny of Caimaninae, using MrBayes version 3.2.6 (Ronquist *et al.* 2012*a*). With the same morphological data matrix used for the parsimony analyses, we performed two independent runs of Markov chain Monte Carlo (MCMC) analyses, using the Mkv model (Markov k-state variable model, with rate variation across characters sampled from a gamma distribution; Lewis 2001). During each run, four chains of 5 million generations were performed. Convergence of both runs was assessed using the potential scale reduction factor (PSRF, with values approaching 1.0 indicating convergence) and average standard deviation of split frequencies (values below 0.01). Trace files were also examined using Tracer version 1.7.1 (Rambaut *et al.* 2018), with effective sample size (ESS) values above 200 indicating that the runs reached a stationary phase.

After the runs, the first 25% of samples were discarded as burn-in and three different consensus tree methods were applied, each one with distinct interpretations of the tree sample and potential implicit issues (O'Reilly & Donoghue 2017). The maximum a posteriori (MAP) tree is the single tree in the posterior sample with the greatest posterior probability; the maximum clade credibility (MCC) tree is the single tree in the posterior with the largest sum of posterior probabilities across all its nodes (Heled & Bouckaert 2013); the majority rule consensus (MRC) tree, also known as half-compatibility tree, displays clades with posterior probability higher than 0.5, collapsing the remaining clades. MAP and MCC trees are fully resolved but may include clades with low posterior probabilities, whereas MRC trees is a conservative approach that might include polytomies (O'Reilly & Donoghue 2017). MRC trees were recovered from the output files of MrBayes, whereas the MCC and MAP trees were obtained using the function `obtainDatedPosteriorTreesMrB()` from the `paleotree` package in R (Bapst 2012; R Core Team 2019). For the MAP tree, the option `MAPosteriori` was used in the argument `outputTrees`.

Finally, additional Bayesian inference analyses were performed after pruning unstable caimanine taxa identified by the IterPCR protocol, maintaining the same model parameters, burn-in factor, and approach for obtaining consensus trees.

Time calibration using the FBD model

The oldest undisputed Caimaninae records are from the Paleocene of South America, with *Necrosuchus ionensis* and *Eocaiman palaeocenicus* from Argentina and *Eocaiman itaboraiensis* from Brazil (Simpson 1937; Bona 2007; Pinheiro *et al.* 2013). However, we have evidence suggesting that these probably do not represent the earliest caimanine lineages. The latest phylogenetic studies (Scheyer *et al.* 2019; Souza-Filho *et al.* 2019; Cidade *et al.* 2020*a*) have consistently found the Neogene taxa *Culebrasuchus mesoamericanus*, *Gnatusuchus pebasensis*, and *Globidentosuchus brachyrostris* as sister (or successively sister) to all other caimanines. Furthermore, a

recent reassessment of *Bottosaurus harlani*, from the Maastrichtian and lower Paleocene of North America, suggests that this taxon might in fact be included within Caimaninae (Cossette & Brochu 2018). Accordingly, it would be interesting to investigate how this topological conformation influences the age constraints of the origin of Caimaninae, as well as the timing of the Caimaninae–Alligatorinae split.

To examine this question and also to obtain a fully time-calibrated phylogeny of Caimaninae, we performed Bayesian tip-dating analyses, using an FBD model (Stadler 2010; Ronquist *et al.* 2012*b*; Heath *et al.* 2014; Zhang *et al*. 2016). For that, we combined temporal information for every taxon in the morphological dataset with the topological constraint obtained from the phylogenetic analyses. Then, we created an empty character matrix using the `createMrBayesTipdatingNexus()` function within the `paleotree` R package (Bapst 2012), which follows the recommendations in Matzke & Wright (2016). A uniform prior was placed on taxon ages, with the extant taxa fixed to 0 and the ages of extinct taxa obtained from the literature. Proportion of sampling of extant taxa (sampleprob) was set to 0.6 (i.e. 16 sampled species; *c.* 60% of 27 currently recognized species; Grigg & Kirshner 2015). A uniform prior was also placed on the age root of the entire tree (i.e. Crocodylia), with maximum and minimum ages set as 145 and 90 Ma, respectively, based on the oldest putative crocodylian record (Mateus *et al.* 2019). Other parameters used default priors assigned by the function. We then used this empty matrix to perform two independent MCMC runs in MrBayes version 3.2.6 (Ronquist *et al.* 2012*a*), with four chains of 25 generations each. As for the phylogeny estimation using Bayesian inference, convergence of both runs was assessed using PSRF and average standard deviation of split frequencies values (with values approaching 1.0 and below 0.01, respectively). After the runs converged, 25% of sampled trees were discarded as burn-in. For reporting the results, only the MRC tree was used.

Body size estimation

Most equations for estimating the body size (total body length, TL) of extinct crocodylomorphs derive from regressed data of extant crocodylian species, using either cranial (Webb & Messel 1978; Hall & Portier 1994; Sereno *et al.* 2001, Hurlburt *et al.* 2003; Platt *et al.* 2009, 2011; Aureliano *et al.* 2015) or postcranial measurements (Farlow *et al.* 2005). Given that the postcranium of *E. cavernensis* is unknown, we decided to estimate TL using an estimation of the cranial length (total cranial length in dorsal view: dorsal cranial length, DCL) of the specimen. We coarsely estimated DCL of *E. cavernensis* by comparing the preserved cranial material of the holotype with complete skulls of other caimanine taxa, extinct and extant. Subsequently, using this estimated DCL, we applied two equations for estimating the TL of *E. cavernensis*. First, we used the equation presented by Hurlburt *et al.* (2003), which is based on morphometric data of multiple modern specimens of *Alligator mississippiensis*. We also used the equations from Aureliano *et al.* (2015), which derive from regressed data of living *Caiman latirostris* specimens (Verdade 2000). More information on body size estimation, including cranial and mandibular measurements of *E. cavernensis*, a full list of specimens used in the comparison, and the regression equations can be found in Godoy *et al.* (2020, supporting information).

Institutional abbreviations. AMNH FARB, Collection of Fossil Amphibians, Reptiles and Birds, American Museum of Natural History, New York, USA; MACN, Museo Argentino de Ciencias Naturales Bernardino Rivadavia, Buenos Aires, Argentina; MCT, Museu de Ciências da Terra, Rio de Janeiro, Brazil; MLP, Museo de La Plata, La Plata, Argentina; MPEF, Museo de Paleontología Egidio Feruglio, Trelew, Argentina; UCPM, University of California Paleontological Museum, California, USA.

SYSTEMATIC PALAEONTOLOGY

CROCODYLIA Gmelin, 1789 (*sensu* Benton & Clark 1988)
ALLIGATOROIDEA Gray, 1844 (*sensu* Brochu 2003)
CAIMANINAE Brochu, 1999 (*sensu* Norell 1988)

Genus EOCAIMAN Simpson, 1933*a*

Type species. Eocaiman cavernensis Simpson, 1933*a*

Eocaiman cavernensis Simpson, 1933*a*

Holotype. AMNH FARB 3158 (Fig. 1), a partial skull and nearly complete mandible, with better preserved left sides. The skull includes the right premaxilla, both maxillae, nasals, the left prefrontal, both lacrimals, the left jugal, both palatines, the left ectopterygoid, the pterygoid bones and a partial left maxillary toothrow. The lower jaw includes both dentaries, the left splenial, the left surangular, and the left angular, as well as a complete left dentary toothrow.

Diagnosis. Caimanine crocodylian diagnosed by the following combination of characters (exclusive features marked with an asterisk): absence of '*canthi rostralii*' and preorbital ridges on the dorsal surface of the maxilla; mediolaterally slender and dorsoventrally low jugal; slender postorbital bar; two small medial jugal foramina, one rostral and another caudal to the

postorbital bar*; rostral processes of the palatines converge medially, forming pointed processes; palatine–pterygoid suture meets the suborbital fenestra at its caudomedial angle (which distinguishes the taxon from *Gnatusuchus pebasensis*); ectopterygoid–pterygoid suture meets the suborbital fenestra at its caudolateral angle; absence of a marked pterygoid lateral process projecting into the ectopterygoid; dorsoventrally slender mandible, bearing 19 dentary teeth; rostrally procumbent dentary teeth (which distinguishes the taxon from all other caimanines for which this region is known, except for *Eocaiman itaboraiensis* and *Gnatusuchus pebasensis*); rostral portion of the dentary (i.e. between the first and the fourth teeth) dorsoventrally lower than at the level of the 11th and the 12th teeth (which distinguishes the taxon from all other caimanines for which this region is known, except for the other two *Eocaiman* species); lateromedially wide and dorsoventrally flat mandibular symphysis; splenial excluded from the mandibular symphysis; mandibular symphysis extends caudally until the fifth dentary alveolus (which distinguishes the taxon from *Eocaiman itaboraiensis*, *Globidentosuchus brachyrostris*, and *Kuttanacaiman iquitosensis*); splenial extended dorsal to the Meckelian groove; rostral processes of the surangular does not bear a spur confining the toothrow; small elliptical external mandibular fenestra; angular–surangular suture meets the external mandibular fenestra near its caudodorsal corner; dentary–angular suture meets the external mandibular fenestra at the ventralmost portion of its margin; rostral teeth crowns circular and pointed, and caudal teeth becoming progressively less pointed and more labiolingually compressed.

Locality and horizon. AMNH FARB 3158 was collected by George G. Simpson and J. Hernández, in 1930, on a cliff (the Gran Barranca, S45° 429 490, W68° 449 160; Fig. 2), south of Lake Colhué Huapí, Chubut Province, Argentina (Simpson 1933*a*; Kay *et al.* 1999). The rocks (*Notostylops* Beds or Simpson's Y Tuff) belong to the Gran Barrancan Member (Sarmiento Formation) and are dated to the Eocene (Bartonian; Ré *et al.* 2010).

DESCRIPTION

This morphological description of *Eocaiman cavernensis* presented is based solely on the type specimen AMNH FARB 3158. When allowed by the preservation of the bones, the cranial and mandibular elements of AMNH FARB 3158 were compared with those of extant and extinct crocodylians with anatomical overlap, particularly with other caimanines. The comparisons were based on first-hand examination and data available from published resources.

The high resolution of the μCT data reveals a clear distinction between trabecular and cortical bone, in both cranial and mandibular bones. Sutures between bones are, in general, easily detected, even though suture morphology is occasionally obscured by cracks and crushed bones. Indeed, the deformation of the material prevents more accurate and detailed description of inner structures, or even the unequivocal detection of structures or bones such as the vomer.

Skull

As described by Simpson (1933*a*), the general aspect of the skull of *Eocaiman cavernensis* (AMNH FARB 3158) resembles that of extant Caimaninae, with a broad and short snout (Figs 1, 3–5). Although the tip of the snout (including the external nares) is not present, the specimen preserves most of the palatal and preorbital regions (for measurements of the preserved material, see Godoy *et al.* 2020, table S1). The skull roof and the occipital region are not preserved. The left side of the skull is better preserved and includes 12 maxillary alveoli, with eight preserved teeth (Figs 4, 5). It also preserves most of the rostral and lateral margins of the orbit, a nearly complete suborbital fenestra and a small portion of the rostrolateral margin of the infratemporal fenestra (Figs 3, 4). The right side of the skull bears only one maxillary tooth (and a partially preserved alveolus); the right orbit, suborbital, and infratemporal fenestrae are missing. The specimen was subjected to compression during the fossilization process, making the left and right sides no longer symmetrically aligned. Some damage and breakage have occurred in the skull roof and palatal region. On the dorsal surface of the skull, dermal bones are ornamented by pits and ridges, which are commonly seen in other crocodylians. These ornamental pits are absent on the ventral surface of the skull (i.e. on the secondary palate), on which only some small foramina are observed lingual to the maxillary toothrow, as well as occlusion pits for the insertion of dentary teeth.

In dorsal view (Fig. 3), the orbits are dorsally oriented and, although not completely preserved, were probably elliptical, narrower rostrally and longer than wide. The preserved portions of the left orbit are delimited rostrolaterally by the lacrimal, rostromedially by the prefrontal, and laterally by the jugal. In ventral view (Fig. 4), the secondary palate is formed by the premaxilla, maxilla, palatine, and pterygoid. The suborbital fenestra is nearly elliptical (i.e. narrower rostrally and longer than wide), bearing a marked lateral expansion on the caudal half of the lateral margin. It is delimited rostrally by the maxilla, medially by the palatine, caudally by the pterygoid, and caudolaterally by the ectopterygoid.

Internally, the nasal passageway can be observed ranging rostrocaudally through most of the extension of the nasals. Its dorsal wall consists mostly of the nasals, whereas the other walls are formed by the maxillae. However, most of the bony walls of the nasal passageway are badly crushed, preventing accurate definition of its limits (either laterally or rostrocaudally). Similarly, due to crushed walls, the paranasal sinus system can be only partially observed, with the two sinuses extending in parallel and lateral to the nasal passageway. The rostralmost extension of the paranasal sinuses reaches, approximately, the level of the sixth maxillary tooth, and their walls presumably comprise the maxillae rostrally and the lacrimals caudally. Deformation of the material makes it difficult to describe or assert the presence of other inner skull cavities, such as the olfactory region of the nasal cavity or the dorsal alveolar canal. More caudal cavities (e.g. nasopharyngeal duct) or endocranial components are not preserved.

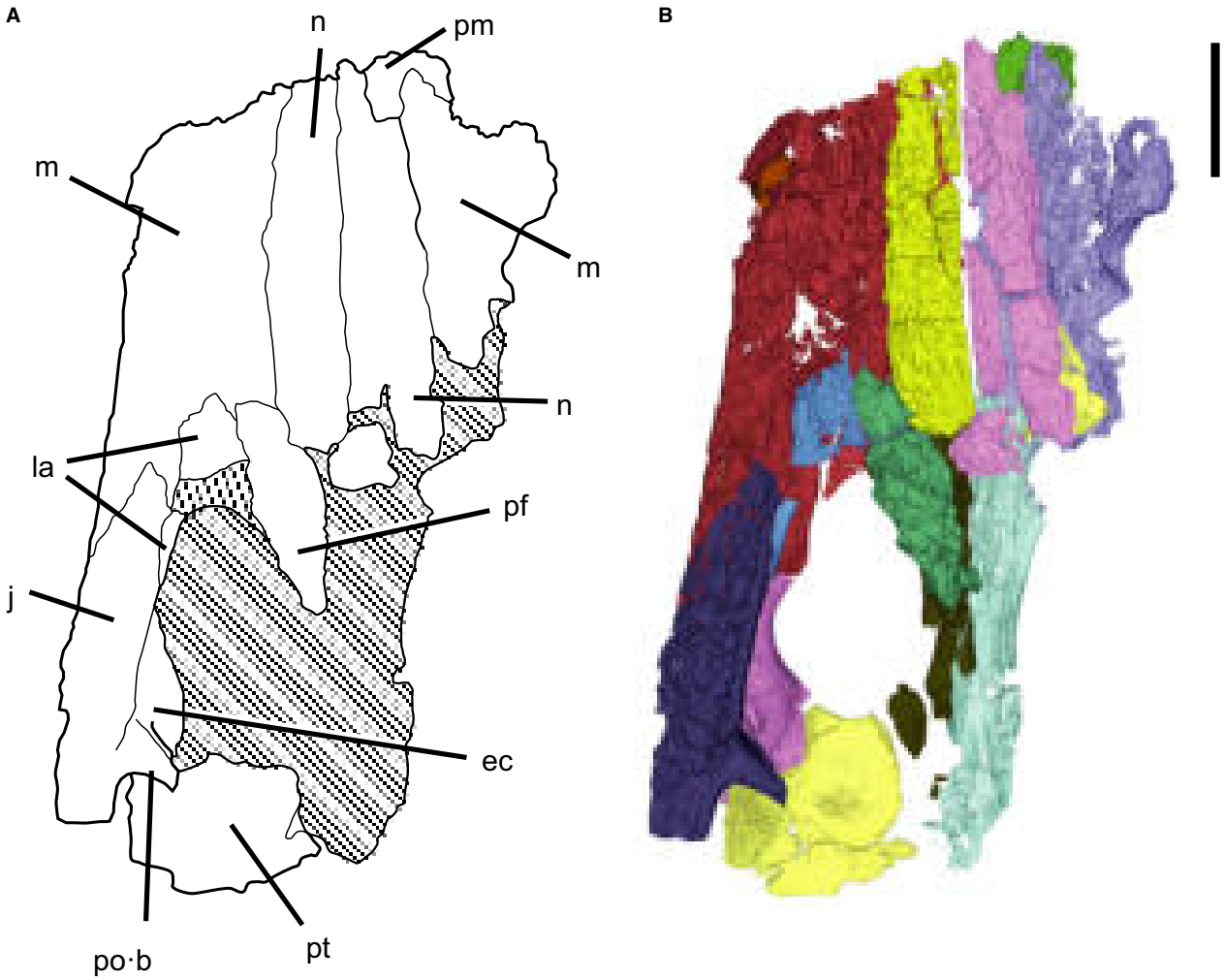

FIG. 3. *Eocaiman cavernensis* (AMNH FARB 3158), dorsal view of the skull. A, drawing of the fossil material. B, 3D surface rendering of individually segmented bones. *Abbreviations*: ec, ectopterygoid; j, jugal; la, lacrimal; m, maxilla; n, nasal; pf, prefrontal; pm, premaxilla; po.b, postorbital bar; pt, pterygoid. Scale bar represents 2 cm.

Premaxilla. Only the caudalmost part the right premaxilla is unequivocally preserved in *Eocaiman cavernensis* (AMNH FARB 3158), with a slightly larger ventral portion forming the palate (Fig. 4). Fragments of the left premaxilla may also be present, but unambiguous identification is hampered by the fragmentary nature of skull region. The external nares and the premaxillary tooth row are not present; thus, no premaxillary teeth are known. The contact with the maxilla is best seen on the ventral surface of the skull (i.e. on the palate), where the short portion of the suture preserved in the specimen extends mediolaterally, perpendicular to the rostrocaudal axis of the skull. In dorsal view, the premaxilla contacts the nasal medially and the maxilla laterally, giving it a triangular shape. Nevertheless, the very fragmentary preservation of the premaxilla obviates further description and comparison of this bone with other caimanines.

Maxilla. Both right and left maxillae are present in *Eocaiman cavernensis* (AMNH FARB 3158). The left element is better preserved, extending rostrocaudally from near the contact with the premaxilla to the contact with the jugal and the ectopterygoid. The left element also preserves most of the maxillary tooth row, bearing 12 continuous alveoli. These possibly represent the sequence from the third to the 14th maxillary alveoli. Eight maxillary teeth are preserved on the left maxilla, although one of these, possibly the fourth maxillary tooth, is visible only in the μCT data. The preservation of the right bone is restricted to its rostromedial portion and only one tooth (probably the third maxillary tooth) is preserved.

The maxilla comprises most of the snout, being the longest bone rostrocaudally and the widest mediolaterally. The μCT data reveal that the maxillary surface within the nasal passageway was probably imperforate, even though the region is fragmentary. In dorsal view (Fig. 3), the maxilla contacts the premaxilla rostrally, the nasal medially, the prefrontal caudomedially, the lacrimal caudally, and the jugal caudolaterally. Although the fragmentary nature of the region prevents a more accurate description, it is very likely that the maxilla did not form part of the orbit, which probably consisted of the prefrontal rostromedially, the lacrimal

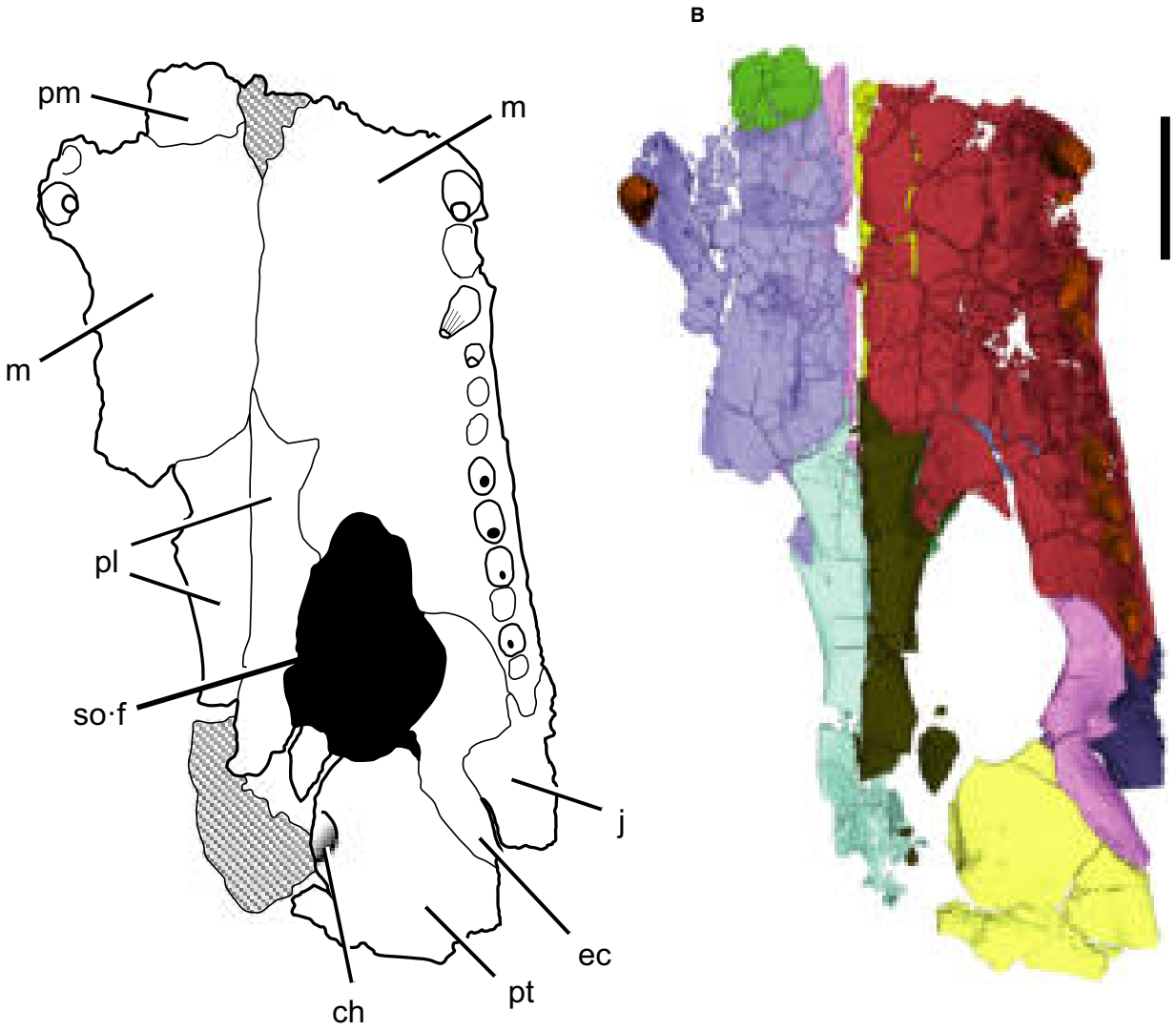

FIG. 4. *Eocaiman cavernensis* (AMNH FARB 3158), ventral view of the skull. A, drawing of the fossil material. B, 3D surface rendering of individually segmented bones. *Abbreviations*: ch, internal choana; ec, ectopterygoid; j, jugal; m, maxilla; pl, palatine; pm, premaxilla; pt, pterygoid; so.f, suborbital fenestra. Scale bar represents 2 cm.

rostrally, and the jugal laterally (other bones possibly participating in the orbital margin, such the frontal and the postorbital, are not preserved, nor their articulation facets with other bones). The lateral margin of the maxilla is straight in dorsal view. There is no evidence of '*canthi rostralii*' on the dorsal surface of the maxilla and the absence of a prominent rostral *canthus* is shared with most caimanines, except for *Purussaurus mirandai*, *P. brasiliensis*, *Melanosuchus niger*, *Caiman latirostris*, *C. brevirostris*, and *C. wannlangstoni* (Brochu 1999; Aguilera *et al.* 2006; Souza-Filho *et al.* 2019). Similarly, it is very likely that preorbital ridges were also absent (even though the poor preservation of this region prevents an unequivocal assessment), a condition shared with all other alligatoroids (Souza-Filho *et al.* 2019).

In ventral view (Fig. 4), the maxilla forms the largest part of the secondary palate. Apart from the rostral contact with the premaxilla, the maxilla also contacts the palatine caudomedially and the ectopterygoid caudolaterally. The maxillary suture with the palatine contacts the rostromedial part of the margin of the suborbital fenestra, whereas the suture with the ectopterygoid contacts the fenestra at the midpoint of its lateral margin. Despite some deformation in the region, we can assert that the maxillary component of the lateral margin of the fenestra is concave, as in *Caiman yacare*, *C. latirostris*, *C. crocodilus*, *C. wannlangstoni*, *Melanosuchus niger*, *Gnatusuchus pebasensis*, and *Kuttanacaiman iquitosensis* (Brochu 1999; Salas-Gismondi *et al.* 2015). The caudalmost extension of the maxilla, where the suture with the ectopterygoid contours the last maxillary alveolus, terminates rostral to the lower temporal bar. Lingual to the linear maxillary toothrow, a deep occlusal pit or groove extends from the third to the sixth preserved alveoli (which probably represent the fifth to the eighth maxillary alveoli). This occlusal groove was probably for the reception of the 12th and 13th dentary teeth.

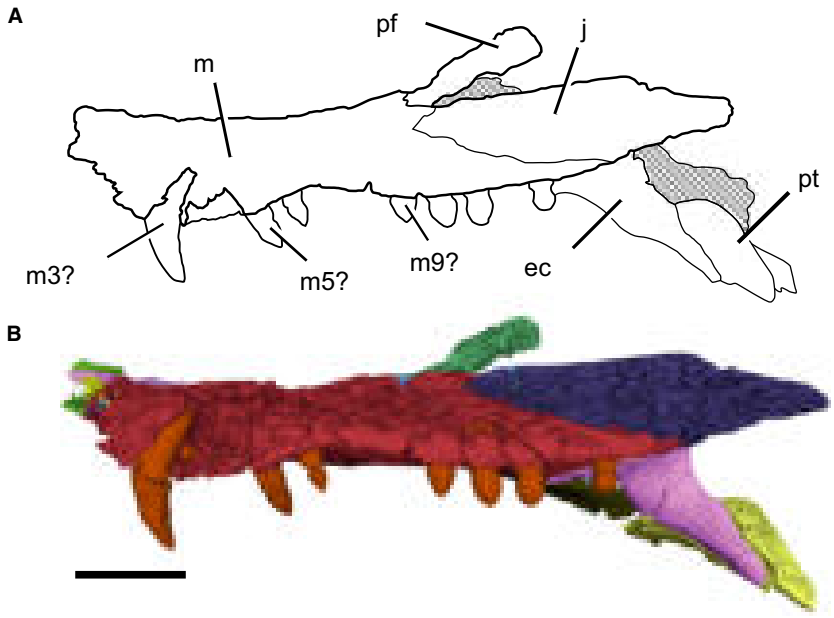

FIG. 5. *Eocaiman cavernensis* (AMNH FARB 3158), left lateral view of the skull. A, drawing of the fossil material. B, 3D surface rendering of individually segmented bones. *Abbreviations*: ec, ectopterygoid; j, jugal; m, maxilla; m3?, putative third left maxillary tooth; m5?, putative fifth left maxillary tooth; m9?, putative ninth left maxillary tooth; pf, prefrontal; pt, pterygoid. Scale bar represents 2 cm.

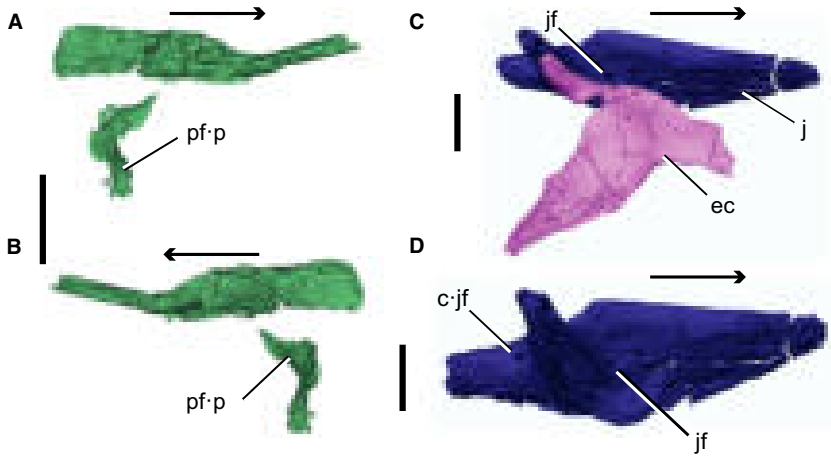

FIG. 6. *Eocaiman cavernensis* (AMNH FARB 3158), detailed cranial morphology illustrated by 3D surface rendering of individually segmented bones. A, prefrontal in medial view. B, prefrontal in lateral view. C, jugal and ectopterygoid in medial view. D, jugal in medial view. Rostral direction is indicated by black arrows. *Abbreviations*: c.jf, caudal jugal foramen; ec, ectopterygoid; j, jugal; jf, jugal foramen; pf.p, prefrontal pillar. Scale bars represent 1 cm.

In lateral view (Fig. 5), the ventral margin of the maxilla extends rostrocaudally in a sigmoidal line. The lowest preserved point coincides with the first preserved alveolus (which also bears the largest preserved tooth and probably represents the third maxillary alveolus). The margin rises dorsally at the level of the fourth preserved alveolus (probably the sixth maxillary alveolus), reaching the highest level at the fifth preserved alveolus, and descending ventrally at the seventh preserved alveolus (probably the ninth maxillary alveolus). Then, the margin continues caudally in a slightly ascending line until the contact with the jugal. Only the caudal contact with the jugal is observed in lateral view.

Nasal. Both nasals are preserved in *E. cavernensis* (AMNH FARB 3158) and can be seen in dorsal view (Fig. 3). The state of preservation is similar in both elements, with the right element being only slightly better preserved rostrally (closer to the contact with the right premaxilla). Despite that, the caudal margin of the external naris cannot be unambiguously identified, so that the participation of the nasals in the naris is uncertain. A

caudal fragment of the right bone is slightly medially displaced, towards the midline of the skull. It is worth mentioning that the illustration in the original description shows this fragment closer to its seemingly natural position (Simpson 1933*a*, fig. 1), suggesting that it was displaced later in time.

Situated on the medial portion of the snout, the nasal is a rostrocaudally elongate bone in dorsal view, similar to that of most alligatoroids (i.e. not as narrow as in most crocodyloids and not as broad and short as in *Purussaurus*; Iordansky 1973; Aguilera *et al.* 2006). Apart from the medial contact with its antimere, the nasal contacts the premaxilla rostrally, the maxilla laterally, and the prefrontal caudolaterally. The absence of any preserved portions of the frontal makes the likely caudal contact of the nasal with this bone unknown. The μCT data show that the nasal did not contact the lacrimal.

Prefrontal. Only a partial left prefrontal is present in *Eocaiman cavernensis* (AMNH FARB 3158). In dorsal view (Fig. 3), it forms the rostromedial margin of the orbit and contacts the nasal rostromedially, the maxilla rostrally, and the lacrimal rostrolaterally. The μCT data also reveal a ventral contact of the prefrontal descending process (i.e. prefrontal pillar) with the palatine (Fig. 6A, B). Although there is a transverse ridge on the dorsal surface of the prefrontal, it is not as abrupt as the prefrontal crests seen in other taxa (e.g. *Purussaurus brasiliensis*, *P. neivensis*, *P. mirandai*, *Acresuchus pachytemporalis*, *Caiman brevirostris*, *C. wannlangstoni*, *Melanosuchus niger* and the extant species of *Caiman*; Souza-Filho *et al.* 2019) and there is no clear evidence that it extended further rostrally along the snout surface. However, the true morphology of this structure cannot be described given the poor preservation of the preorbital region. The same applies to the possible absence of knob-like processes on the prefrontal dorsal surface adjacent to the margin of the orbit, which cannot be unequivocally assessed. Similarly, the possible medial contact between prefrontals cannot be verified given the absence of a right element and of the frontal bone.

The right prefrontal pillar is partially preserved and could be visualized using the μCT data (Fig. 6A, B). The medial process of the prefrontal pillar is rostrocaudally expanded and wide at the base, as in all other caimanines in which these features can be accessed (i.e. mostly extant taxa; Brochu 1999). However, given that the pillar is not entirely preserved, it is not possible to confirm whether it was a solid structure or contained a pneumatic recess.

Lacrimal. Although not unequivocally identifiable by direct observation in dorsal view, the μCT data reveal that both lacrimals are present in *E. cavernensis* (AMNH FARB 3158; Fig. 3). The left element is better preserved, with a larger fragmented portion rostral to the orbit, as well as a smaller isolated fragment that lies more caudally, at the lateral margin of the orbit. The right bone is preserved only as some fragments, rostral to the orbit. The μCT data also reveal that the lacrimal extends as a thin lamina beneath portions of the maxilla, nasal and prefrontal.

The lacrimal comprises most of the rostral margin of the orbit and contacts the maxilla rostrally and rostrolaterally, the jugal caudolaterally, and the prefrontal medially. The absence of a lacrimal–nasal contact is shared with other extinct caimanines, such as *Purussaurus neivensis*, *P. mirandai*, *Mourasuchus amazonensis*, and *Kuttanacaiman iquitosensis* (Price 1964; Aguilera *et al.* 2006; Salas-Gismondi *et al.* 2015). However, the condition in *E. cavernensis* seems to differ from that of all these taxa, given that both a rostral extension of the prefrontal and a caudal projection of the maxilla prevents the contact between lacrimal and nasal. Nevertheless, the poor preservation of the preorbital region, on both sides of the skull, prevents unequivocal description of the condition in *E. cavernensis*.

Jugal. Only the left jugal is preserved in *E. cavernensis* (AMNH FARB 3158), missing its caudalmost portion (caudal to the postorbital bar). The jugal is mediolaterally slender and dorsoventrally low, as in all caimanines, except for *Mourasuchus amazonensis* and *M. pattersoni* (Cidade *et al.* 2017). In dorsal view (Fig. 3), it forms most of the lateral margin of the orbit, which extends rostrocaudally in an almost straight line and does not bear the typical notch seen in *Gavialis gangeticus* (Brochu 1999). The jugal also partially defines the caudal limit of the orbit, due to the dorsomedial projection of the jugal portion of postorbital bar. Given that the jugal is not completely preserved, only a small rostrolateral portion of the lower temporal bar is observed. In addition to the contacts with the maxilla and lacrimal, rostrally and rostromedially, respectively, the jugal also contacts the ectopterygoid along the ventromedial portion of the postorbital bar, and the suture with this bone extends rostrally on the medial surface of the jugal (Fig. 6C).

A slender postorbital bar is shared with all other alligatoroids (Norell 1988; Brochu 1999). Although only the ventralmost portion of the bar is preserved, it is possible to observe its ventral margin inset from the lateral jugal surface, as in all other caimanines (Brochu 1999). The jugal bears a small medial foramen rostral to the postorbital bar (Fig. 6C), as in all other caimanines, except for *Globidentosuchus brachyrostris* and *Bottosaurus harlani* (Scheyer *et al.* 2013; Cossette & Brochu 2018). Another clearly visible foramen, of similar size, is seen on the jugal medial surface, caudal to the bar (Fig. 6D).

Palatine. Both palatines are preserved in *E. cavernensis* (AMNH FARB 3158), both lacking only their caudalmost portions. In ventral view (Fig. 4), the palatine is a rostrocaudally elongate bone forming most of the convex medial margin of the suborbital fenestra. Apart from the rostral contact with the maxilla and the dorsal contact with the prefrontal (seen on μCT), the palatines also contact one another medially. Furthermore, the palatine probably also contacted the pterygoid caudolaterally, although the fragmentary nature of this region prevents assessment of the true condition of this suture.

The broad rostral process of the palatine extends beyond the rostral margin of the suborbital fenestra, as in all other alligatoroids (Brochu 1999). The rostralmost tips of the rostral processes of both palatines converge medially to form a pointed process. This rostral process also shows another, more laterally pointed projection, but the condition in *E. cavernensis* is different from the notch in *Paleosuchus* (Brochu 1999). A small part of the rostralmost portion of the lateral edge of the palatine projects into the suborbital fenestra, but the condition is more subtle than the large projections seen in *Paleosuchus* and

Kuttanacaiman iquitosensis (Brochu 1999; Salas-Gismondi *et al.* 2015). More caudally, the lateral edge of the palatine extends in an almost straight rostrocaudal line and then flares laterally to form the caudomedial margin of the suborbital fenestra. Although the region is poorly preserved, the palatine–pterygoid contact probably occurred near the caudomedial angle of the fenestra, as in all caimanines, except for *Gnatusuchus pebasensis* (Brochu 1999; Salas-Gismondi *et al.* 2015). However, the contribution of the palatine to the internal choana is unknown.

Ectopterygoid. The left ectopterygoid is nearly completely preserved in *E. cavernensis* (AMNH FARB 3158). In ventral view (Fig. 4), it forms the strongly bowed caudal half of the lateral margin of the suborbital fenestra, contacting the maxilla rostrally and the pterygoid caudomedially. The ectopterygoid also contacts the jugal dorsally, forming the ventral portion of the lateral part of the postorbital bar (Fig. 6C). However, it is not possible to determine if the ectopterygoid extended along the medial face of the bar.

In ventral view (Fig. 4), the rostralmost tip of the ectopterygoid tapers to a point at the lateral margin of the suborbital fenestra, as in all other alligatoroids (Brochu 1999). The contact with the maxilla extends caudally in a laterally convex curve, differing from the overall straight suture seen in living caimanines. The suture between these two bones approaches the maxillary toothrow only at the level of the last alveolus (possibly the 14th maxillary alveolus). Therefore, the ectopterygoid does not enclose the toothrow, a condition similar to all other alligatoroids (Brochu 1999). The contact with the pterygoid occurs at the caudolateral angle of the fenestra and there is no sign of a pterygoid flexure. The absence of a marked pterygoid lateral process projecting into the ectopterygoid of *E. cavernensis* is inferred here based on the possible sutural marks seen on μCT, even though that exact region is broken. The absence of this feature is shared only with *Gnatusuchus pebasensis* among caimanines (Brochu 1999; Salas-Gismondi *et al.* 2015). The pterygoid ramus of the ectopterygoid does not extend to the caudalmost portion of the pterygoid, as in all crocodylians (Brochu 1999).

Pterygoid. Only the left pterygoid is preserved in *E. cavernensis* (AMNH FARB 3158), lacking its medial portion and its caudolateral tip. In ventral view (Fig. 4), the preserved portion of the bone is nearly as rostrocaudally elongate as it is lateromedially wide. The pterygoid contributes to a significant portion of the caudal margin of the suborbital fenestra, contacts the ectopterygoid rostrolaterally and possibly the palatine rostromedially. The internal choana is partially preserved, with the pterygoid unequivocally contributing to its lateral and caudal margins. The choana lies closer to the caudal margin of the suborbital fenestra than to the caudalmost portion of the pterygoid and was possibly projected rostroventrally, but a more precise description is precluded by the fragmentary nature of the region. The pterygoid flange dorsally encloses the ectopterygoid caudalmost portion.

Mandible

The mandible of *Eocaiman cavernensis* (AMNH FARB 3158) is dorsoventrally slender and both hemimandibles are present (Figs 7, 8). Whereas the right side preserves only the dentary and 11 dentary teeth, the left one has all 19 dentary teeth preserved on a nearly complete dentary, as well as partial splenial, surangular and angular bones. The coronoid and the articular bones are not preserved on either side, preventing the description of the retroarticular process and the glenoid fossa.

The lateral and ventral surfaces of the lower jaws are ornamented with pits and grooves not seen on the medial surface, whereas the dorsal surface has a series of occlusion pits labial to the tooth row between the third and the 13th alveoli. In lateral view, an elliptical external mandibular fenestra is delimited by the dentary rostrally, the surangular dorsally, and the angular caudoventrally. The fenestra is not enlarged as in the *Purussaurus* species and *Acresuchus pachytemporalis*, in which the large size of the fenestra exposes the foramen intermandibularis caudalis in lateral view (Aguilera *et al.* 2006; Souza-Filho *et al.* 2019).

Dentary. Both dentaries are preserved in *Eocaiman cavernensis* (AMNH FARB 3158; Figs 7, 8). The left element is nearly complete, whereas the right bone lacks both the rostralmost (rostral to the second dentary alveolus) and the caudalmost (caudal to the 13th alveolus) portions. The rostralmost tip of the left dentary, bearing the first two dentary teeth, was attached to the remainder of the mandible after the original description by Simpson (1933*a*). Indeed, this small portion of the dentary remained isolated from the holotype mandible until at least 2006 (M. Ellison, pers. comm. January 2014), which explains why some previous studies do not mention, figure or use morphological information from this piece (Brochu 1999, 2011; Bona 2007; Pinheiro *et al.* 2013), in contrast to more recent works (e.g. Bona & Barrios 2015). The left dentary preserves 19 teeth, whereas 11 teeth are preserved on the right element (from the third to the 13th dentary tooth). Simpson (1933*a*) suggested the presence of a 20th dentary alveolus on the left hemimandible, caudal to the last preserved tooth, an assertion subsequently supported by Pinheiro *et al.* (2013). However, this hypothesis is rejected here, based on the μCT data.

The dentary comprises most of each hemimandible, especially in lateral view, as in all crocodylians (Iordansky 1973). In dorsal view (Fig. 7), the dentary contacts the splenial medially and the surangular caudally. In lateral view (Fig. 8A, B), apart from the caudodorsal contact with the surangular, it is also possible to observe the caudoventral contact with the angular. The dentary forms the rostral margin of the external mandibular fenestra in lateral view (Fig. 8A, B), as well as the rostral half of the dorsal margin of the fenestra. Because the region is damaged, the exact position at which the dentary–surangular suture contacted the dorsal margin of the fenestra is unknown, but it most certainly occurred rostral to the caudodorsal corner of the fenestra, as in all caimanines (Brochu 1999, 2011).

In lateral view (Fig. 8A, B), the dorsal margin of the dentary extends caudally in a sinusoidal line, starting rostrally at its ventralmost point between the first and the fourth dentary teeth, reaching its dorsalmost point at the level of the 13th dentary tooth, and then descending ventrally through the last dentary teeth. The rostral portion of the dentary (i.e. between the first

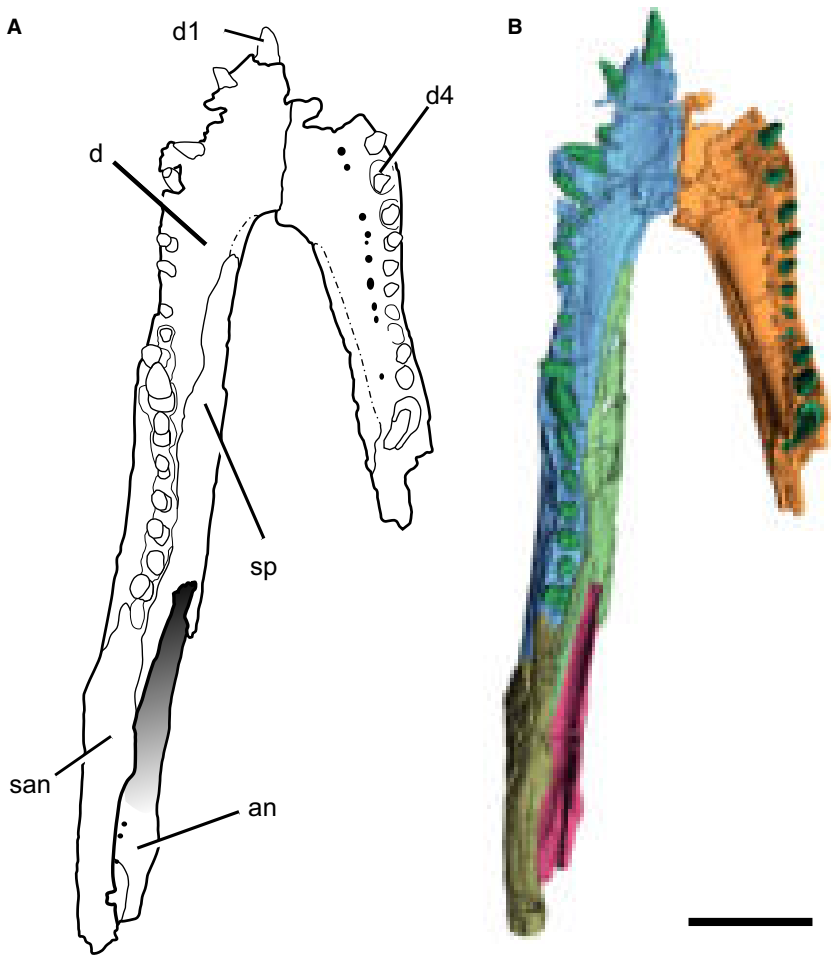

FIG. 7. *Eocaiman cavernensis* (AMNH FARB 3158), dorsal view of the lower jaws. A, drawing of the fossil material. B, 3D surface rendering of individually segmented bones. *Abbreviations*: an, angular; d, dentary; d1, first dentary tooth; d4, fourth dentary tooth; san, surangular; sp, splenial. Scale bar represents 2 cm.

and the fourth teeth) is dorsoventrally lower than at the level of the 11th and the 12th teeth. This condition is also observed in *Eocaiman palaeocenicus* and was proposed by Bona (2007) as a diagnostic feature for the genus *Eocaiman*. Subsequently, Pinheiro *et al.* (2013) described the same condition for all three mandibular specimens of *E. itaboraiensis*. However, the holotype of *E. itaboraiensis* (MCT 1791-R) seems to bear a slightly different morphology, with the rostral portion of the dentary relatively elevated in relation to the other *Eocaiman* taxa. Therefore, although in our character matrix we have followed the scorings of Pinheiro *et al.* (2013) for this character, closer examination of the *E. itaboraiensis* specimens is still needed to confirm its morphology and perhaps its validity.

The lateromedially wide, dorsoventrally flat symphyseal region of *Eocaiman cavernensis* consists solely of the dentary, without the participation of the splenial, and extends caudally until the fifth dentary alveolus (Fig. 7). The extension of the symphyseal region is very plastic among caimanines, encompassing only the first dentary alveolus (in *Mourasuchus amazonensis* and *Mourasuchus atopus*; Langston 1965; Cidade *et al.* 2019*a*), up to the 11th alveolus (in *Gnatusuchus pebasensis*; Salas-Gismondi *et al.* 2015). However, most caimanines share the condition seen in *Eocaiman cavernensis*, with the symphysis extending back to the level of the fifth tooth (e.g. in the *Purussaurus*, *Caiman* and *Paleosuchus* species, as well as in *Melanosuchus niger*, *Bottosaurus harlani*, *Necrosuchus ionensis*, *Acresuchus pachytemporalis*, *Centenariosuchus gilmorei* and *Tsoabichi greenriverensis*; Iordansky 1973; Brochu 1999, 2010, 2011; Aguilera *et al.* 2006; Hastings *et al.* 2013; Cossette & Brochu 2018; Souza-Filho *et al.* 2019; Cidade *et al.* 2020*a*). Among other *Eocaiman* species, the condition is unknown in *E. palaeocenicus*, given that the symphysis reaches the fifth alveolus on the left hemimandible of the holotype (MPEF-PV 1933), but seems to extend beyond that level on the right hemimandible, suggesting some degree of taphonomic distortion in the region (Bona 2007). Finally, the symphysis extends to the sixth dentary alveolus in all three mandibular specimens of *E. itaboraiensis* (MCT 1791-R, MCT 1792-R, MCT 1793-R; Pinheiro *et al.* 2013).

Splenial. Only the left splenial is preserved in *Eocaiman cavernensis* (AMNH FARB 3158), which is very fragmented, lacking its rostralmost portion. In dorsal view (Fig. 7), the splenial contacts the dentary laterally and the surangular caudolaterally. In medial view (Fig. 8C, D), it also contacts the angular caudoventrally. The splenial does not contribute to the

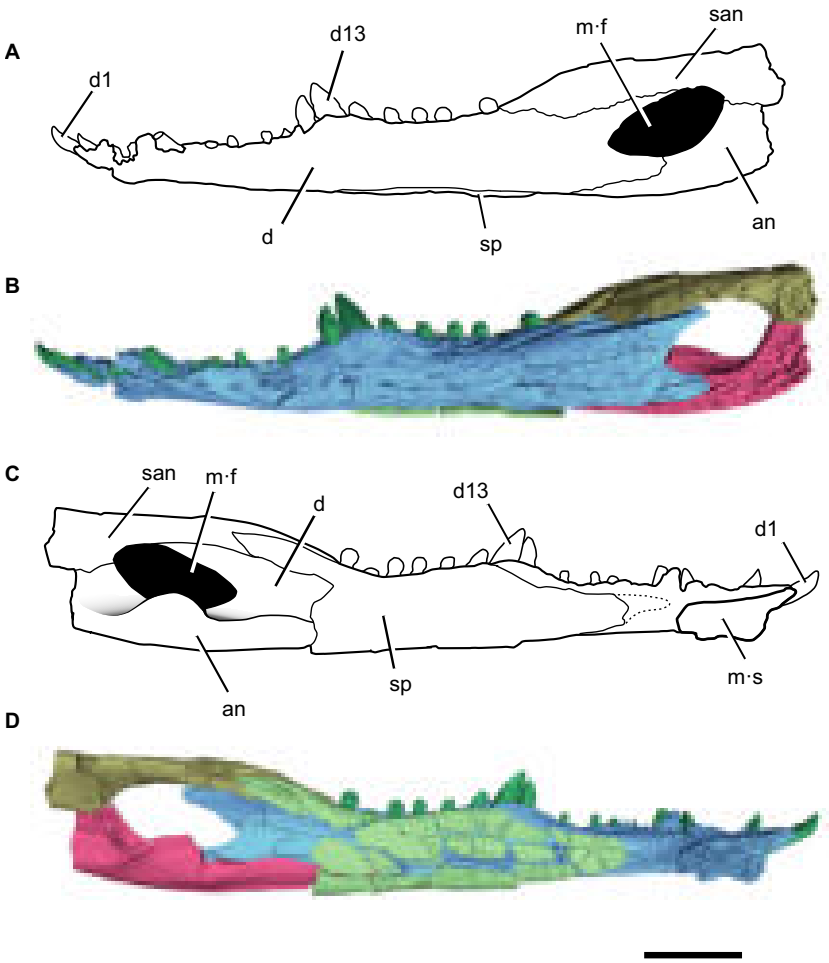

FIG. 8. *Eocaiman cavernensis* (AMNH FARB 3158), lateral and medial views of the lower jaws. A, drawing of the fossil material, in left lateral view. B, 3D surface rendering of individually segmented bones, in left lateral view. C, drawing of the fossil material, left hemimandible in medial view. D, 3D surface rendering of individually segmented bones, left hemimandible in medial view. *Abbreviations*: an, angular; d, dentary; d1, first dentary tooth; d13, 13th dentary tooth; m.f, external mandibular fenestra; m.s, mandibular symphysis; san, surangular; sp, splenial. Scale bar represents 2 cm.

mandibular symphysis and, although its rostral portion is absent, on μCT the sutural scars clearly show that its rostral tip extended dorsal to the Meckelian groove. This condition is seen in all other caimanines, except for those in which the splenial participates in the symphysis (i.e. *Globidentosuchus brachyrostris* and *Gnatusuchus pebasensis*; Scheyer *et al.* 2013; Salas-Gismondi *et al.* 2015). Although the original description of *Eocaiman itaboraiensis* suggests a participation of the splenial in the mandibular symphysis of this taxon (Pinheiro *et al.* 2013), we agree with Cidade *et al.* (2020*a*) in which an accurate assessment is hampered by the fragmentary nature of the known specimens. The intermandibular foramina (oralis, medialis, and caudalis) are either not completely preserved or cannot be fully distinguished in *Eocaiman cavernensis* (AMNH FARB 3158).

Surangular. The left surangular is preserved in *Eocaiman cavernensis* (AMNH FARB 3158), missing its caudalmost portion. In lateral view (Fig. 8A, B), it forms the caudal half of the dorsal margin of the external mandibular fenestra and contacts the dentary rostroventrally, and the angular caudoventrally. In medial view (Fig. 8C, D), it meets the splenial rostrally, the dentary rostroventrally and the angular caudoventrally. Regarding the rostral processes of the surangular, the dorsal element extends rostrally to the level of the last dentary alveolus in dorsal view (Fig. 7), but does not show the spur that confines the toothrow seen in *Caiman yacare* and *Caiman crocodilus* (Brochu 1999). The ventral process, however, is not completely preserved in *Eocaiman cavernensis*, hampering further assessment. In lateral view (Fig. 8A, B), the angular–surangular suture contacts the external mandibular fenestra near its caudodorsal corner. A suture passing broadly along the ventral margin of the fenestra was initially proposed as a synapomorphy of Caimaninae (Brochu 1999; Hastings *et al.* 2016). However, in agreement with recent reassessment (Cidade *et al.* 2020*a*), on reinterpretation, most caimanines display the angular–surangular suture meeting the fenestra at the caudodorsal angle.

Angular. Only the left angular is preserved in *Eocaiman cavernensis* (AMNH FARB 3158), missing its caudalmost portion. In lateral view (Fig. 8A, B), it contacts the dentary rostrally and the surangular caudodorsally, and forms the caudoventral margin of the external mandibular fenestra. The dentary–angular suture meets the external mandibular fenestra at its ventralmost portion, and extends rostroventrally to the ventral

surface of the mandible. In medial view (Fig. 8C, D), the angular also meets the splenial rostrally and forms the floor of a partially preserved adductor fossa. Still in medial view, only the ventral margin of the foramen intermandibularis caudalis is preserved. In dorsal view, the dorsal surface of the angular within the adductor fossa bears a series of four small foramina medial to the external mandibular fenestra.

Dentition

Most alveoli of *Eocaiman cavernensis* (AMNH FARB 3158) are circular on cross-section. As in other caimanines, the teeth have well-defined and non-serrated carinae, with smooth apicobasal striae (best visible on the dentary teeth). The rostral tooth crowns are circular in cross-section and apically pointed, becoming progressively less pointed caudally (i.e. with more rounded apices). Caudal teeth are also slightly compressed labiolingually, although not as much as in *Paleosuchus*, *Bottosaurus harlani* and *Kuttanacaiman iquitosensis* (Brochu 1999; Salas-Gismondi *et al.* 2015; Cossette & Brochu 2018).

Maxillary teeth. The 12 alveoli preserved on the left maxilla of *Eocaiman cavernensis* (AMNH FARB 3158) are inferred to represent the third to the 14th maxillary alveoli. In that case, the fourth maxillary tooth would be the largest, as in all caimanines except for *Culebrasuchus mesoamericanus*, *Gnatusuchus pebasensis*, and *Purussaurus brasiliensis* (Hastings *et al.* 2013; Salas-Gismondi *et al.* 2015). This is based on the alveolar size, given that just a small part of this tooth (potentially a replacement tooth) is preserved and seen only on μCT. However, because the toothrow is not completely preserved, the relative size of maxillary teeth cannot be confirmed. More caudal teeth are, in general, smaller, less pointed, and slightly more compressed labiolingually. As in all other crocodylians, the diameter of the penultimate maxillary alveolus is not much larger than that of the last one (Brochu 1999).

Dentary teeth. Eocaiman cavernensis is the only species of the genus with a completely known dentary toothrow, which is preserved on the left dentary of AMNH FARB 3158. This toothrow preserves 19 alveoli and bears, at least partially, all dentary teeth. The first dentary tooth is large and procumbent, a condition shared only with *Eocaiman itaboraiensis* and *Gnatusuchus pebasensis* within caimanines (Pinheiro *et al.* 2013; Salas-Gismondi *et al.* 2015). From the second to the 10th dentary tooth, teeth are slightly inclined rostrally, a condition that differentiates *E. cavernensis* from the other two species of the genus (even though two specimens of *E. itaboraiensis*, MCT 1792-R and MCT 1793-R, have a similar morphology; Pinheiro *et al.* 2013). The fourth is the largest dentary tooth in *Eocaiman cavernensis*. As in all caimanines, except for *Gnatusuchus pebasensis* (Salas-Gismondi *et al.* 2015), the alveoli for the third and fourth dentary teeth are not confluent in *Eocaiman cavernensis* (Brochu 1999). More caudally, the second largest dentary tooth is the 13th. An enlarged 13th or 14th tooth is a condition shared only with *Necrosuchus ionensis* among caimanines (Brochu 2011; Cidade *et al.* 2020*a*). *Globidentosuchus brachyrostris* also has enlarged 13th and 14th teeth, but this taxon is distinct from the former two by exhibiting a series of large alveoli caudal to the 14th alveolus (Scheyer *et al.* 2013; Cidade *et al.* 2020*a*). Caudal to the 13th alveolus, the dentary teeth of *Eocaiman cavernensis* become increasingly smaller, less pointed and slightly compressed labiolingually, as also seen in more caudal maxillary teeth.

PHYLOGENETIC ANALYSIS

Phylogenetic affinities of Eocaiman cavernensis *and other caimanines*

The morphological reassessment of *Eocaiman cavernensis* performed here allowed the scoring of a total of 37 characters for this taxon in our modified version of the matrix of Cidade *et al.* (2020*a*). This represents an improvement of nearly 40% in relation to the original, in which *Eocaiman cavernensis* was scored for only 27 characters. In total, the states of 17 characters were altered, whereas 3 characters previously scored were changed to unscored (for details about rescorings, see Godoy *et al.* 2020).

The maximum parsimony analysis using the complete data matrix recovered 185 520 MPTs of 646 steps (consistency index [CI] = 0.384, retention index [RI] = 0.808). The strict consensus (Godoy *et al.* 2020, fig. S1) shows a large polytomy formed by the ingroup taxa, within which only a few crocodylian subgroups are found as monophyletic, such as Crocodyloidea, Alligatorinae (with minimal Bremer supports), and Gavialoidea (Bremer = 3). These results are in contrast to those of Cidade *et al.* (2020*a*), who used a similar version of our matrix (the major source of differences is the rescorings of *Eocaiman cavernensis* performed here) and found a better resolved strict consensus. Furthermore, Bayesian inference analysis with the same matrix also yielded poorly resolved MRC trees (Godoy *et al.* 2020, fig. S2), which is the consensus tree approach that shows only clades with posterior probability of more than 50%. Even though the MRC tree recovers clades not present in the strict consensus from the parsimony analysis, such as Hylaeochampsidae and Diplocynodontinae, a large polytomy is seen at the base of Alligatoroidea, hampering the recognition of clades within it.

Given the poor resolution using both maximum parsimony and Bayesian approaches, we applied the IterPCR protocol to identify unstable taxa. Of these, three putative caimanines were recognized as major sources of instability: *Protocaiman peligrensis*, *Necrosuchus ionensis*, and *Eocaiman itaboraiensis*. These taxa are known from poorly preserved or incomplete specimens, and the uncertainty related to

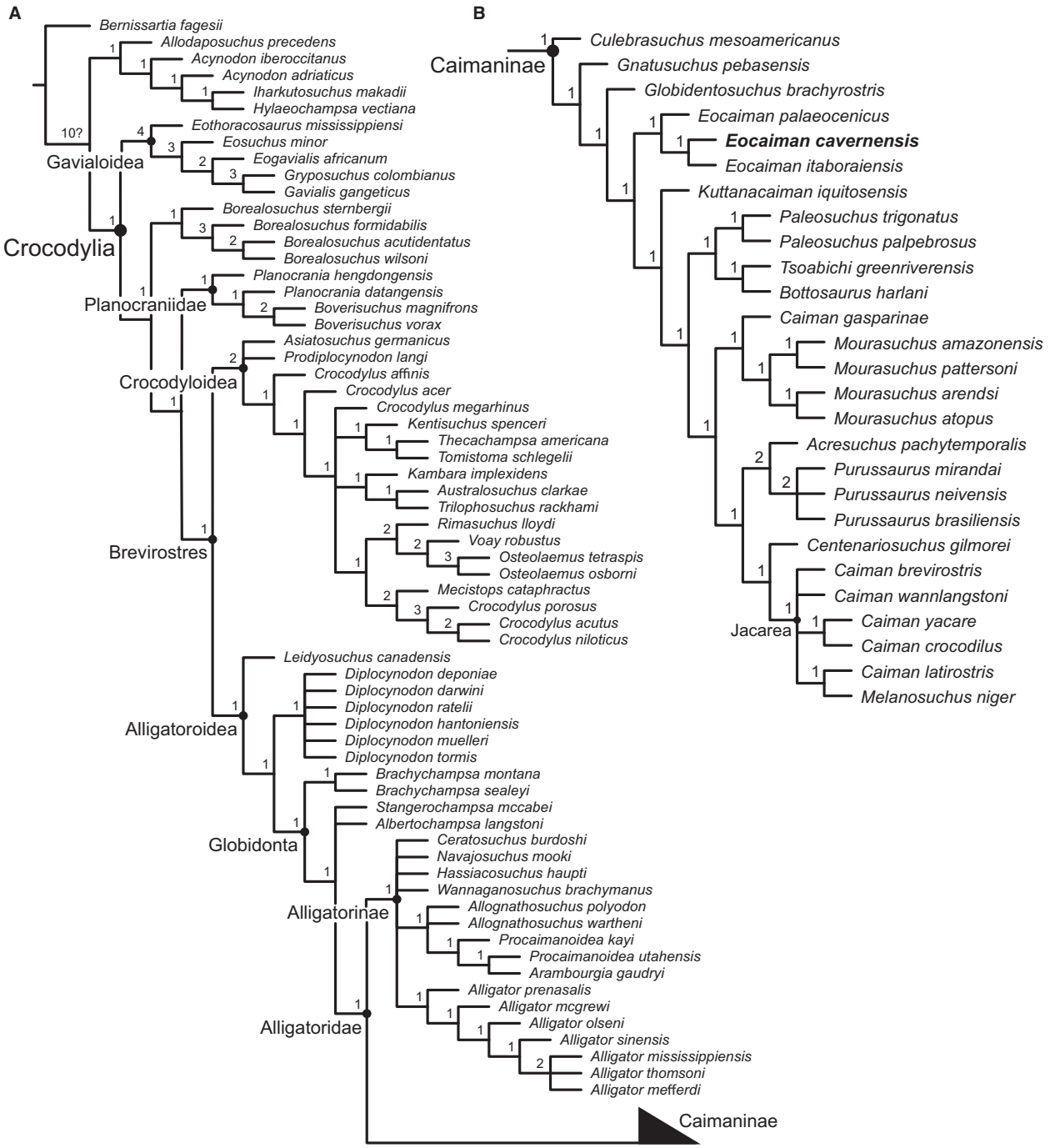

FIG. 9. Strict consensus of the 480 most parsimonious trees of the maximum parsimony analysis after the removal of *Protocaiman peligrensis* and *Necrosuchus ionensis* from the dataset. A, entire crocodylian tree. B, relationships within Caimaninae, highlighting the position of *Eocaiman cavernensis*. Numbers above nodes indicate Bremer support values.

them is probably due to the large amount of missing data instead of character conflict. Consequently, the IterPCR results show many alternative positions for these three taxa (results of the IterPCR procedure are provided in Godoy *et al.* 2020). *Protocaiman peligrensis* has *c.* 14% of its characters scored in our matrix (27 out of 187 characters), and was found either within planocraniids or among the *Diplocynodon* species (see IterPCR results in Godoy *et al.* 2020). This is consistent with the MAP and MCC trees from the Bayesian analysis, which recovered this taxon in similar positions (Godoy *et al.* 2020, figs S3, S4), but is in strong contrast to the results presented by Bona *et al.* (2018), who

found *Protocaiman peligrensis* within Caimaninae, a position never found in any of the analyses conducted here. *Necrosuchus ionensis* has the same number of characters scored in our matrix (27), and the IterPCR results show alternative positions within Caimaninae, similar to what was recovered in both MAP and MCC (see IterPCR results and Godoy *et al.* 2020, figs S3, S4). Finally, *Eocaiman itaboraiensis* has only 6 characters scored (*c.* 3%), and the instability of this taxon is illustrated by the highly contrasting alternative positions recovered for it in the IterPCR results, either within Caimaninae or outside Crocodylia (see IterPCR results in Godoy *et al.* 2020). A non-crocodylian position for this taxon is also suggested by the results of the Bayesian inference analysis (using any of the consensus trees; Godoy *et al.* 2020, figs S2–S4).

We then decided to run additional phylogenetic analyses without these highly unstable taxa. However, given that the relative phylogenetic position of *Eocaiman itaboraiensis* is important for assessing the monophyly of the genus *Eocaiman*, we opted for not excluding this taxon from any of our phylogenetic analyses. Therefore, we ran three additional maximum parsimony analyses: one without *Protocaiman peligrensis*, another without *Necrosuchus ionensis*, and a third excluding both taxa. Finally, we also ran one extra Bayesian inference analysis, using a matrix without both *Protocaiman peligrensis* and *Necrosuchus ionensis*.

The first additional parsimony analysis, excluding only *Protocaiman peligrensis*, yielded only slightly improved results in relation to the original analysis (27 960 MPTs of 643 steps; CI = 0.386, RI = 0.809), given that the strict consensus still shows a large polytomy at the base of the ingroup clade (Godoy *et al.* 2020, fig. S5). This suggests a high degree of instability for *Necrosuchus ionensis* (and/or *Eocaiman itaboraiensis*), which is consistent with previous work (Cidade *et al.* 2020*a*) and our IterPCR results (Godoy *et al.* 2020).

The second additional analysis, excluding only *Necrosuchus ionensis*, shows a better scenario, with a reduced number of MPTs (3360 MPTs, 645 steps; CI = 0.384, RI = 0.808) and a better resolved strict consensus (Godoy *et al.* 2020, fig. S6). Apart from Gavialoidea (Bremer = 5) and Crocodyloidea (Bremer = 2), monophyletic Caimaninae and Alligatorinae are also recovered (both with minimum Bremer support), forming a resolved Alligatoridae (Bremer = 1). Globidonta is not recovered as monophyletic in the strict consensus, given the presence of a polytomy at the base of Brevirostres, formed by Alligatoridae, Crocodyloidea, *Leidyosuchus canadensis*, *Protocaiman peligrensis*, and the species of *Diplocynodon*, *Planocrania*, and *Boverisuchus*. Uncertainty regarding the position of *Protocaiman peligrensis* is interesting because, despite its high degree of incompleteness, this taxon possesses mosaic features, associated with both caimanines and non-alligatorid globidontans (i.e. *Brachychampsa*, *Albertochampsa* and *Stangerochampsa*). For instance, it exhibits some putative caimanine synapomorphies (e.g. the presence of foramina on the medial parietal wall of supratemporal fenestra), but also shows an overall skull roof configuration that resembles that of taxa closely related to *Brachychampsa*, with a broad skull roof and relatively large supratemporal fenestrae (Bona *et al.* 2018; Cidade *et al.* 2020*a*). This combination of features in *Protocaiman peligrensis* possibly contributed to the phylogenetic results seen in Bona *et al.* (2018), who found the lineage of Cretaceous North American taxa (i.e. *Brachychampsa* and related forms) within Caimaninae, as the sister group of a clade formed by *Protocaiman peligrensis* and all other caimanines (Bona *et al.* 2018). This arrangement is not found here, but further discoveries, particularly in North America, might elucidate the early evolution of caimanines.

Finally, the third additional parsimony analysis, without both *Protocaiman peligrensis* and *Necrosuchus ionensis*, was much more informative, with 480 MPTs (642 steps; CI = 0.386, RI = 0.809). The strict consensus (Fig. 9) is almost fully resolved, with all typically recognized crocodylian subgroups recovered as monophyletic (e.g. Gavialoidea, Brevirostres, Crocodyloidea, Alligatoroidea, Globidonta, Alligatorinae and Caimaninae). Arrangements within these groups are the same or very similar to that of recent parsimony analyses using previous versions of this dataset (Souza-Filho *et al.* 2019; Cidade *et al.* 2020*a*). Furthermore, Bayesian inference analysis with this reduced version of the matrix (i.e. without *Protocaiman peligrensis* and *Necrosuchus ionensis*) also shows slightly improved results in relation to the analysis using the complete matrix, with the MRC tree recovering Caimaninae (with a posterior probability of 0.53) and some other alligatoroid subgroups (Godoy *et al.* 2020, fig. S7). However, compared with the maximum parsimony analysis, Bayesian inference provided relatively poorer results, therefore we primarily focus on the parsimony results (i.e. the strict consensus tree) when describing the phylogenetic relationships within Caimaninae, even though some results of the Bayesian analysis are also mentioned.

The parsimony strict consensus shows a monophyletic Caimanine (Fig. 9), with minimum Bremer support. A single character supports the monophyly of caimanines, which is a large supraoccipital exposure on the dorsal skull table, with the parietal excluded from the caudal edge of table (159: 0 → 3). The inclusiveness of Caimaninae is consistent with nearly all contemporary phylogenetic studies (e.g. Cidade *et al.* 2017, 2020*a*, *b*; Cossette & Brochu 2018; Souza-Filho *et al.* 2019), only differing from the work of Bona *et al.* (2018), which found *Brachychampsa* and other closely related North American taxa within the clade, as well as *Protocaiman peligrensis* (which was consistently recovered outside Caimaninae here).

Within Caimaninae, *Culebrasuchus mesoamericanus* is recovered as the sister taxon to all other members of the

group, with *Gnatusuchus pebasensis* and *Globidentosuchus brachyrostris* successively more nested in the group (Fig. 9). Apart from the studies that used a very similar version of our matrix (i.e. Cidade *et al.* 2017, 2020*a*, *b*; Souza-Filho *et al.* 2019), which found the same arrangement regarding *Culebrasuchus mesoamericanus*, *Gnatusuchus pebasensis* and *Globidentosuchus brachyrostris*, the placement of *Culebrasuchus mesoamericanus* as sister to all other caimanines was also previously found by Cossette & Brochu (2018) and Hastings *et al.* (2013), whereas some studies placed the taxon within Alligatorinae (Salas-Gismondi *et al.* 2015; Hastings *et al.* 2016; Bona *et al.* 2018). Our Bayesian inference analysis does not provide consistent results either. On the one hand, the MCC tree places these three taxa among caimanines, with the same arrangement of our parsimony results (although Caimaninae was recovered with a posterior probability of only 13%; Godoy *et al.* 2020, fig. S9). On the other hand, the MRC tree found *Gnatusuchus* and *Globidentosuchus* within Caimaninae, but *Culebrasuchus* was placed in a polytomy at the base of Alligatoroidea (Godoy *et al.* 2020, fig. S7). The MAP tree shows a similar scenario, with *Culebrasuchus* within Alligatorinae (Godoy *et al.* 2020, fig. S8).

Successively sister to the crown-group caimanines are *Kuttanacaiman iquitosensis* and the clade formed by the three *Eocaiman* species (Fig. 9). *Kuttanacaiman iquitosensis* as the sister taxon of crown-group Caimaninae is consistent with recent analyses (Bona *et al.* 2018; Souza-Filho *et al.* 2019; Cidade *et al.* 2020*a*), and is supported by caudal teeth labiolingually compressed (79: 0 → 1) and a marked pterygoid lateral process (ectopterygoid–pterygoid flexure) projecting into the ectopterygoid (125: 0 → 1).

A monophyletic *Eocaiman* (Fig. 9) was also recovered by Pinheiro *et al.* (2013), as well as other recent studies that

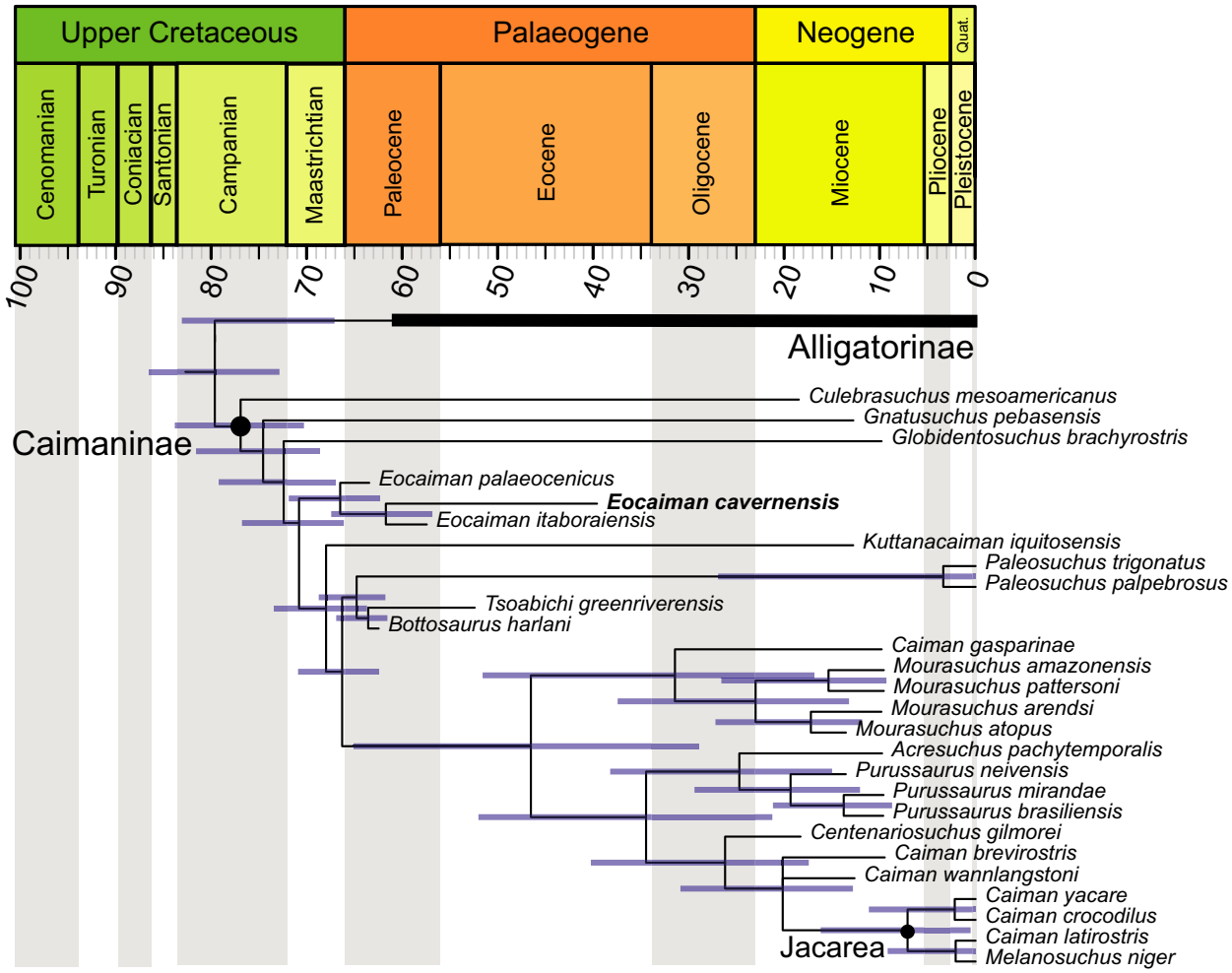

FIG. 10. Time-calibrated phylogeny of Caimaninae represented by a reduced version of the majority rule consensus (MRC) tree recovered from Bayesian analysis using the fossilized birth–death model. *Necrosuchus ionensis* was manually excluded from the MRC tree after the analysis. Blue bars indicate 95% highest posterior density age ranges of nodes.

included all three species (i.e. Cidade *et al.* 2017, 2020*a*, *b*; Souza-Filho *et al.* 2019). The only exception is Bona *et al.* (2018), who found the *Eocaiman* species in an unresolved clade with *Notocaiman stromeri* (this later taxon was not included in our data matrix due to its very incomplete preservation). The single synapomorphy supporting a monophyletic *Eocaiman* is the rostral portion of the dentary (between the first and the fourth teeth) dorsoventrally lower than at the level of the 11th and 12th teeth (183: 0 → 1). Within *Eocaiman*, *E. palaeocenicus* is sister to the clade formed by the other two species, which is supported by the presence of procumbent dentary teeth (48: 1 → 0). Bayesian inference does not provide further support for a monophyletic *Eocaiman*, given that none of the consensus trees (MRC, MAP and MCC trees) found this arrangement (Godoy *et al.* 2020, figs S7–S9). Indeed, the only species of the genus consistently found in our Bayesian analysis within Caimaninae was *E. palaeocenicus*, whereas *E. cavernensis* was frequently found among alligatorines and *E. itaboraiensis* was recovered outside Crocodylia.

Crown caimanines are recovered as a clade in the strict consensus (Fig. 9), supported by three synapomorphies: mandibular symphysis extending to fourth or fifth dentary alveolus (49: 1 → 0); maxilla with linear medial margin adjacent to suborbital fenestra (111: 1 → 0); and upturned dorsal edges of the orbits (136: 0 → 1). Within crown caimanines, *Bottosaurus harlani* is recovered as sister to *Tsoabichi greenriverensis* (Fig. 9), and these two taxa form a clade with the *Paleosuchus* species, as in Cidade *et al.* (2020*a*), in a better resolved arrangement than that found by Cossette & Brochu (2018). The clade formed by *Bottosaurus harlani*, *Tsoabichi* and *Paleosuchus* is supported by four unambiguous synapomorphies. Bayesian inference provides further support for this arrangement, given that all consensus trees recover this clade with more than 70% posterior probability (Godoy *et al.* 2020, figs S7–S9). It is worth mentioning that we did not include *Bottosaurus fustidens* (Cossette 2020) in our analyses, because its description was published shortly before the submission of the present study.

Similar to the findings of Cidade *et al.* (2020*a*), our results show *Caiman gasparinae* as the sister group of the clade formed by the four *Mourasuchus* species (Fig. 9), in contrast to the results from Bona *et al.* (2012), who found this taxon within Jacarea (i.e. the node-based group including the last common ancestor of *Caiman crocodilus*, *C. yacare*, *C. latirostris*, and *Melanosuchus niger* and all of its descendants; Brochu 1999). In our analysis, this arrangement is supported by a single synapomorphy: the nasals excluded from the external naris (82: 1 → 2). Given that this region of the skull is very fragmentary in the type and only specimen of *C. gasparinae*, further assessment might elucidate whether or not this corresponds to the correct morphological interpretation. The MCC tree of our Bayesian analysis (Godoy *et al.* 2020, fig. S9) also recovered *C. gasparinae* as sister to *Mourasuchus*, even though with relatively low posterior probability (0.28).

As in Souza-Filho *et al.* (2019), and Cidade *et al.* (2020*a*), *Acresuchus pachytemporalis* is recovered as the sister taxon of the *Purussaurus* species (Fig. 9), an arrangement supported by three synapomorphies: presence of a large external mandibular fenestra, with most of the foramen intermandibularis caudalis visible in lateral view (63: 1 → 2); rostral tip of frontal forming an acute point (130: 1 → 0); and dermal bones of skull roof overhanging the margin of a large and oval supratemporal fenestra (151: 1 → 3). We found a sister taxon relationship between the clade formed by *Acresuchus* and *Purussaurus* and the *Centenariosuchus gilmorei* + Jacarea clade, which is supported by four synapomorphies: dorsal margin of iliac blade rounded, with modest dorsal indentation (34: 3 → 1); teeth circular in cross-section (79: 1 → 0); concavo-convex frontoparietal suture (150: 1 → 0); and presence of preorbital crest (186: 0 → 1). This result is consistent with what was found recently by Souza-Filho *et al.* (2019) and Cidade *et al.* (2020*a*), differing from previous studies, which frequently recovered a closer relationship between *Mourasuchus* and *Purussaurus* (Salas-Gismondi *et al.* 2015; Bona *et al.* 2018), sometimes forming a clade with the North American taxon *Orthogenysuchus olseni* (Pinheiro *et al.* 2013; Hastings *et al.* 2013, 2016). *Orthogenysuchus* was not included in the present analysis because this taxon is currently being reassessed after further preparation of the type specimen revealed new features and possible reinterpretations (PLG pers. obs.; Salas-Gismondi *et al.* 2015).

Centenariosuchus gilmorei is recovered as the sister taxon of a monophyletic Jacarea (Fig. 9), which in turn is not fully resolved, but formed by *Melanosuchus niger* and five *Caiman* species (*C. wannlangstoni*, *C. brevirostris*, *C. latirostris*, *C. crocodilus*, *C. yacare*). This position for *Centenariosuchus gilmorei* was recovered in previous studies (Bona *et al.* 2018; Souza-Filho *et al.* 2019; Cidade *et al.* 2020*a*) and is supported here by an incisive foramen projecting between the first premaxillary teeth (89: 0 → 2). Regarding our Bayesian analysis, the MCC tree recovered *Centenariosuchus gilmorei* in a similar position, sister to a clade formed by *Melanosuchus* and those five *Caiman* species (Godoy *et al.* 2020, fig. S9), even though with a low posterior probability (0.11).

DISCUSSION

Caimaninae evolution and biogeography in a temporal context

The topological constraint used for the time calibration analysis was essentially that of the strict consensus of the

maximum parsimony analyses without *Protocaiman* and *Necrosuchus* (Fig. 9). The only difference was that we have manually included (i.e. using Mesquite; Maddison & Maddison 2018) *Protocaiman* and *Necrosuchus* in the strict consensus topology based on the alternative positions indicated by the IterPCR results (Godoy *et al.* 2020). Therefore, *Protocaiman* was included in a polytomy at the base of the clade formed by Brevirostres and Planocraniidae, whereas *Necrosuchus* was included in a polytomy at the base of the clade formed by *Eocaiman* and *Kuttanacaiman* + crown caimanines.

Our results indicate that the origin of Caimanine is constrained between 83.86 and 70.34 Ma (95% highest posterior density, HPD; median = 76.97 Ma), a range that extends from the Santonian to the Maastrichtian (see Fig. 10 for a reduced consensus tree; the complete time-calibrated tree is available as a supplementary Newick file in Godoy *et al.* 2020). A slightly older age (86.47–72.76 Ma; median = 79.75 Ma) was estimated for the Caimaninae–Alligatorinae split. Apparently, the current topological conformation, with the oldest lineages not represented by the oldest records (i.e. with long ghost lineages close to the base), did not generate significant temporal uncertainty regarding the origin of caimanines and the Caimaninae–Alligatorinae split. Comparatively, there are other nodes within Caimaninae with much higher uncertainty (i.e. longer 95% HPD ranges), such as the split between the two *Paleosuchus* species, as well as the node formed by the *Mourasuchus* species and *Caiman gasparinae* (Fig. 10).

A possible Campanian origin for Caimaninae is consistent with the oldest known record of a putative crocodylian: *Portugalosuchus azenhae*, from the late Cenomanian of Portugal (*c.* 95 Ma; Mateus *et al.* 2019). Although not included in our analyses, this taxon is *c.* 10 myr older than the oldest age estimated by our analyses for Caimaninae. Among recent efforts to obtain a time-calibrated phylogeny for caimanines or crocodylians, Bona *et al.* (2018) found an older (Coniacian) age for Caimaninae using the minimum branch length (mbl) method. However, such as other a posteriori time-calibration methods (*sensu* Lloyd *et al.* 2016), the mbl method has been criticized for relying solely on occurrence data and suffering from arbitrary choices and assumptions (Bapst 2014; Lloyd *et al.* 2016). Other studies obtained divergence times for Crocodylia using only molecular data, including Oaks (2011) and the recently published work of Pan *et al.* (2020). These two studies found the most recent common ancestor of all living caimanines to be much younger (Eocene and Oligocene–Miocene, respectively) than our estimates for Caimaninae, even for crown caimanines (70.95–62.55 Ma; median = 66.34 Ma). This can be explained by either the complete absence of information from fossils (i.e. in the case of Pan *et al.* 2020) or the omission of some recently discovered taxa in node-dating analyses (i.e. in the case of Oaks 2011). Finally, Lee & Yates (2018) used total evidence (i.e. with both molecular and morphological data) tip-dating analyses and found a slight younger age for Caimaninae (Danian–Selandian) compared with the present results. This is consistent if we consider the recent reassessment of *Bottosaurus harlani* as a caimanine, given that this Late Cretaceous taxon was included in our analyses but not in those of Lee & Yates (2018).

The above results can serve as an important tool for analysing and interpreting the complex biogeographical scenario during the early evolution of caimanines, an issue already addressed by previous studies (Hastings *et al.* 2013; Bona *et al.* 2018). The oldest unambiguous records of South American caimanines come from the Paleocene of Argentina and Brazil (*Eocaiman palaeocenicus*, *E. itaboraiensis* and *Necrosuchus ionensis*; Cidade *et al.* 2019*b*), as well as the two putative caimanines *Protocaiman peligrensis* and *Notocaiman stromeri* (Bona *et al.* 2018), this last taxon not included in our analyses due to its fragmentary nature. Except for *E. itaboraiensis*, all of these are from the Patagonian area of Argentina, located in the south of the continent. Likewise, according to nearly all recent phylogenetic analyses (Scheyer *et al.* 2019; Cidade *et al.* 2020*a*), the known representatives of the earliest divergent caimanine lineages (i.e. *Culebrasuchus*, *Gnatusuchus* and *Globidentosuchus*) are also from South or Central America. Finally, almost all living caimanines are found only in South America today, with the only exception being *Caiman crocodilus*, which extends its range to southern Mexico (Grigg & Kirshner 2015).

However, this seemingly entirely South and Central American history has been challenged by recent quantitative investigations of the historical biogeography of Caimaninae, which indicated a North American origin for the group (Hastings *et al.* 2013; Bona *et al.* 2018). These studies used probabilistic methods, which are highly sensitive to topological constraints, but the predominantly North American fossil record of Alligatorinae (the sister taxon of caimanines) provides support for these results. Accordingly, a first dispersal event from North to southern South America occurred early in the evolution of Caimaninae, probably in the Late Cretaceous according to our time-calibrated tree (Fig. 10). The fact that the oldest and southernmost South American records for the group (from the Paleocene of Patagonia) do not currently represent the earliest divergent caimanine lineages (which are from the Miocene of Panama and the Amazonian region) predicts the presence of ghost lineages and an unknown Late Cretaceous and Paleocene caimanine diversity in Central America and northern South America.

As suggested by previous quantitative studies (Hastings *et al.* 2013; Bona *et al.* 2018), there were probably other important biogeographic events during the evolution of Caimaninae, including other dispersal events between North and South America. Among these is the case of the only two putative North American caimanines, *Tsoabichi greenriverensis* and *Bottosaurus harlani*, which are found as sister taxa in our analyses and form a clade with the two species of *Paleosuchus* (Fig. 9), in agreement with previous results (Cossette & Brochu 2018; Cidade *et al.* 2020*a*; Cossette 2020). This is interesting given both the ages and the distribution of these four taxa. Whereas *Paleosuchus* is extant and found only in South America, *Tsoabichi* is from the Eocene and *Bottosaurus harlani* from the Maastrichtian–Paleocene of North America. The difference in age between these North American taxa and *Paleosuchus* can probably explain the very long age range of the split between the two *Paleosuchus* species, of more than 20 myr (95% HPD range = 26.95–0.002 Ma; median = 3.38 Ma). Furthermore, if further studies confirm the phylogenetic position for *Bottosaurus harlani*, it would represent the oldest known record of Caimaninae, providing further support for a North American origin of the group. In this context, *Tsoabichi* could be understood as a remnant representative of the same lineage, as well as the newly described *Bottosaurus fustidens*, from the late Paleocene of North America (Cossette 2020), which was not included in the present study. Indeed, this would also suggest that many of the early cladogenetic events of the evolutionary history of caimanines took place in a relatively short period of time, across the K–Pg boundary, and possibly in the northern portions of the palaeogeographical distribution of the group.

Body size and palaeoecology of Eocaiman cavernensis

After comparing the cranial measurements of *E. cavernensis* to that of multiple caimanine specimens (for details, see Godoy *et al.* 2020, supporting information), we coarsely estimated a DCL ranging from 16.05 to 27.67 cm. Given the significant variation between these estimates, which illustrates a high diversity of cranial lengths and shapes in the group, we used the average value (20.69 cm) for applying the equations to estimate total body size (i.e. TL). Using the equation of Hurlburt *et al.* (2003), we estimated a TL for *Eocaiman cavernensis* of 1.59 m, whereas using the equations of Aureliano *et al.* (2015) we estimated a TL of 1.78 m, with 95% confidence intervals between 1.53 and 2.07 m (see Godoy *et al.* 2020 for details). It is worth mentioning that the dataset used by Aureliano *et al.* (2015) for obtaining the equations includes only juvenile or subadult specimens of *Caiman latirostris* (Verdade 2000), which may generate overestimations.

Nevertheless, we can be confident that this individual was unlikely to have exceeded 2.5 m in total size. These values would suggest that *E. cavernensis* was comparable in size to most living caimanine species (Grigg & Kirshner 2015). The two *Paleosuchus* species are considered to be the smallest caimanines, reaching no more than 2.3 m (*Paleosuchus palpebrosus* is the smallest extant caimanine, at up to 2.1 m; Sanaiotti *et al.* 2010; Grigg & Kirshner 2015), whereas the three *Caiman* species have maximum sizes of *c.* 2–2.5 m. Given that among extant caimanines only *Melanosuchus niger* can be regarded as a large crocodylian (reaching up to 4 m; Grigg & Kirshner 2015), the current scenario might suggest that Caimaninae would represent the lineage with the smallest species within Crocodylia. However, the fossil record for the group includes some of the largest taxa known to date, not only among crocodylians, but also when considering all crocodylomorphs (Godoy *et al.* 2019). The Miocene genera *Purussaurus* and *Mourasuchus* are widely known for being gigantic, safely reaching more than 5 m in total length (Price 1964; Langston 1965, 2008; Aguilera *et al.* 2006, Aureliano *et al.* 2015; Cidade *et al.* 2017; Scheyer *et al.* 2019). In particular, the largest known specimen of *Purussaurus brasiliensis* could have reached more than 12 m (Aureliano *et al.* 2015). Furthermore, *Acresuchus pachytemporalis* and *Bottosaurus harlani* were also large-bodied taxa (probably reaching more than 3 m; Cossette & Brochu 2018; Souza-Filho *et al.* 2019). At the other extreme, *Tsoabichi greenriverensis* and *Eocaiman itaboraiensis* were much smaller species, at nearly 1 m in total length (Brochu 2010; Pinheiro *et al.* 2013).

This high variability in body size observed within Caimaninae is reflected in the high degree of ecological diversity displayed by its members. As with other living crocodylians, modern caimanines are generalist carnivores. Dietary preferences vary along ontogeny, with juveniles tending to prey on insects, small fishes and crustaceans, whereas adults usually add larger fishes, birds, and mammals to their diet (Grigg & Kirshner 2015). Presumably, analogous diets can be proposed for many extinct taxa, mainly those with similar dentition and reaching larger sizes (including *Purussaurus*, *Acresuchus*, and *Bottosaurus harlani*; Aureliano *et al.* 2015; Souza-Filho *et al.* 2019). In contrast, some other extinct species (such as *Globidentosuchus brachyrostris*, *Gnatusuchus pebasensis*, *Kuttanacaiman iquitosensis*, *Caiman wannlangstoni*, and *Caiman brevirostris*) were small-bodied animals displaying variable degrees of crushing dentition, probably adapted for a durophagous diet (Scheyer *et al.* 2013; Fortier *et al.* 2014; Salas-Gismondi *et al.* 2015). Among living taxa, blunter teeth are also seen in adult specimens of *Caiman latirostris*, the diet of which includes snails (Ősi & Barrett 2011; Ősi 2014). Additionally, the peculiar morphology of *Mourasuchus*, including a very long, broad and flattened

snout, indicates a feeding behaviour that deviates from that of most crocodylians (Langston 1965, 2008), with suggestions including filter-feeding and gulp-feeding strategies (Bona *et al.* 2013; Cidade *et al.* 2019*c*).

In the case of *Eocaiman cavernensis*, the dentition with sharper teeth rostrally and blunter ones caudally resembles that seen in some extant caimanines, suggesting a generalist feeding habit that may have included small vertebrates and invertebrates (i.e. molluscs and crustaceans). However, given the strongly procumbent rostral dentary teeth of *E. cavernensis*, as well as the rostral part of the dentary being at a relatively lower level than the caudal portion, different strategies have been previously suggested for the taxon. Among these, a 'bottom-scooping' foraging behaviour was hypothesized (Cidade & Hsiou 2018), similar to the 'shovelling' behaviour proposed for *Gnatusuchus pebasensis* (Salas-Gismondi *et al.* 2015). Regardless of the specificities of *Eocaiman cavernensis* feeding strategies, a semi-aquatic habit is consistently inferred for the taxon. This lifestyle would be also compatible with its cranial morphology (e.g. dorsoventrally low rostrum, dorsal position of the orbits, and dentition), as well as with the climate of Patagonia during the Paleocene and the Eocene, which was probably significantly more humid and warmer than today, supporting the existence of more abundant vegetation and water bodies (Báez & Gasparini 1977; Albino 1993; Gasparini 1996).

CONCLUSIONS

Eocaiman cavernensis is an important representative of Caimaninae, a group of predominately South and Central American crocodylians. During the last decades, this Eocene taxon from southern Argentina has been included in multiple phylogenetic analyses, but a more detailed morphological assessment was lacking. Here, we present a redescription of the type specimen of *Eocaiman cavernensis* (AMNH FARB 3158) based on close examination of the fossil material and μCT data. This allowed us to reinterpret some aspects of the specimen's morphology and to subsequently reassess the phylogenetic relationships within Caimaninae. Our initial maximum parsimony results yielded a poorly resolved strict consensus, which was caused by the presence of highly unstable taxa, such as *Protocaiman peligrensis*, *Necrosuchus ionensis* and *Eocaiman itaboraiensis*. This was consistent with the Bayesian inference analysis and the IterPCR results, which located these taxa in alternative positions across the crocodylian phylogeny. Then, another set of analyses (without some highly unstable taxa) provided much improved results. We found a monophyletic *Eocaiman* genus and recovered *Culebrasuchus mesoamericanus* as the sister taxon to all other caimanines. Our results do not support the inclusion of the North American globidontans (i.e. taxa closely related to *Brachychampsa*) within Caimaninae. Additionally, we provide a time-calibrated tree of Caimaninae (for the first time using an FBD model), which can serve as a basis for future quantitative analyses (i.e. biogeographical and other phylogenetic comparative methods) on the group. Our results indicate a Campanian origin for Caimaninae (*c.* 75 Ma), which suggests that a dispersal event from North to southern South America occurred early in the evolution of the group, possibly during the Late Cretaceous. Finally, we also estimate the total body length of *Eocaiman cavernensis* as not more than 2.5 m, which is about the size of most living caimanines. *Eocaiman cavernensis* was probably a semi-aquatic taxon, whereas the presence of rostral procumbent teeth in the lower jaws, as well as that of blunter teeth more caudally, suggests a generalist diet, possibly associated with a bottom-scooping behaviour in rivers, lakes, and other aquatic environments.

Acknowledgements. Access to fossil and herpetological collections was possible thanks to Carl Mehling (AMNH), David Kizirian (AMNH), Lauren Vonnahme (AMNH), Pat Holroyd (UCMP), Marcelo Reguero (MLP), Stella Alvarez (MACN), and Rodrigo Machado (MCT). We thank Gabriel Ferreira and José Luis Carballido (MPEF) for photographs of *Eocaiman palaeocenicus*. We thank Henry Towbin and Mick Ellison (AMNH) for assistance with μCT and photography of the studied specimen, respectively. Alan Turner, Andrew Moore, Felipe Pinheiro, Gabriel Ferreira, Thiago Marinho and Estevan Eltink are further thanked for assistance with segmentation of the specimen, phylogenetic analyses and discussion at different stages of this study. We further thank the editor Stephan Lautenschlager for handling the manuscript, as well as Sally Thomas and two anonymous reviewers for their constructive comments. PLG was supported by Fundação de Amparo à Pesquisa do Estado de São Paulo (FAPESP; grant numbers: 2011/16007-9 and 2013/06811-0), University of Birmingham and Coordenação de Aperfeiçoamento de Pessoal de Nível Superior (CAPES; grant number: 3581-14-4), and the National Science Foundation (NSF DEB grant number: 1754596). GMC was supported by Conselho de Desenvolvimento Científico e Tecnológico (CNPq; grant number: 140808/2016-7), CAPES (finance code 001), and FAPESP (grant number: 2013/04516-1). MAN was supported by the Division of Paleontology at the AMNH and the Macaulay Family endowment. TNT is made freely available through the Willi Henning Society.

DATA ARCHIVING STATEMENT

The μCT data for this study, including the tiff stacks (slices) and mesh files (in .ply format), are available via MorphoSource: http://www.morphosource.org/Detail/MediaDetail/Show/media_id/63541
Data supporting this study, including the data matrix, results of IterPCR procedure, the complete time-calibrated MRC tree from the Bayesian analysis and a list of DOIs for MorphoSource μCT data for

AMNH FARB 3158, as well as additional notes and results, are available in the Dryad Digital Repository: https://doi.org/10.5061/dryad.xsj3tx9bt

Editor. Stephan Lautenschlager

REFERENCES

AGUILERA, O. A., RIFF, D. and BOCQUENTIN-VILLANUEVA, J. 2006. A new giant *Purussaurus* (Crocodyliformes, Alligatoridae) from the Upper Miocene Urumaco formation, Venezuela. *Journal of Systematic Palaeontology*, **4**, 221–232.

ALBINO, A. M. 1993. Snakes from the Paleocene and Eocene of Patagonia (Argentina): paleoecology and coevolution with mammals. *Historical Biology*, **7**, 51–69.

AMEGHINO, F. 1906. Les formations sédimentaires du Crétacé supérieur et du Tertiaire de Patagonie avec un parallele entre leurs faunes mammalogiques et celles de l'ancien continent. *Anales del Museo Nacional de Buenos Aires*, **8**, 1–568.

AURELIANO, T., GHILARDI, A. M., GUILHERME, E., SOUZA-FILHO, J. P., CAVALCANTI, M. and RIFF, D. 2015. Morphometry, bite-force, and paleobiology of the Late Miocene Caiman *Purussaurus brasiliensis*. *PLoS One*, **10**, e0117944.

BÁEZ, A. M. and GASPARINI, Z. B. 1977. Origen y evolución de los anfibios y reptiles del Cenozoico de América del Sur. *Acta Geológica Lilloana*, **14**, 149–232.

BAPST, D. W. 2012. paleotree: an R package for paleontological and phylogenetic analyses of evolution. *Methods in Ecology & Evolution*, **3**, 803–807.

—— 2014. Assessing the effect of time-scaling methods on phylogeny-based analyses in the fossil record. *Paleobiology*, **40**, 331–351.

BELLOSI, E. S. 2010. Physical stratigraphy of the Sarmiento formation (middle Eocene–lower Miocene) at Gran Barranca, central Patagonia. 19–32. *In* MADDEN, R. H., CARLINI, A. A., VUCETICH, M. G. and KAY, R. F. (eds) *The paleontology of Gran Barranca: Evolution and environmental change through the middle Cenozoic of Patagonia*. Cambridge University Press.

BENTON, M. J. and CLARK, J. M. 1988. Archosaur phylogeny and the relationships of the Crocodylia. 295–338. *In* BENTON, M. J. (ed.) *The phylogeny and classification of the tetrapods*. Clarendon Press, Oxford.

BONA, P. 2007. Una nueva especie de *Eocaiman* Simpson (Crocodylia, Alligatoridae) del Paleoceno Inferior de Patagonia. *Ameghiniana*, **44**, 435–445.

—— and BARRIOS, F. 2015. The Alligatoroidea of Argentina: an update of its fossil record. 143–158. *In* FERNÁNDEZ, M. and HERRERA, Y. (eds) *Reptiles extintos: Volumen en Homenaje a Zulma Gasparini*. Publicación Electrónica de la Asociación Paleontológica Argentina, Buenos Aires, Argentina.

—— RIFF, D. and GASPARINI, Z. B. 2012. Late Miocene crocodylians from northeast Argentina: new approaches about the austral components of the Neogene South American crocodylian fauna. *Earth & Environmental Science Transactions of the Royal Society of Edinburgh*, **103**, 551–570.

—— DEGRANGE, F. J. and FERNÁNDEZ, M. S. 2013. Skull anatomy of the bizarre crocodylian *Mourasuchus nativus* (Alligatoridae, Caimaninae). *The Anatomical Record*, **296**, 227–239.

—— EZCURRA, M. D., BARRIOS, F. and FERNANDEZ BLANCO, M. V. 2018. A new Palaeocene crocodylian from southern Argentina sheds light on the early history of caimanines. *Proceedings of the Royal Society B*, **285**, 20180843.

BREMER, K. 1988. The limits of amino acid sequence data in angiosperm phylogenetic reconstruction. *Evolution*, **42**, 795–803.

—— 1994. Branch support and tree stability. *Cladistics*, **10**, 295–304.

BROCHU, C. A. 1999. Phylogenetics, taxonomy, and historical biogeography of Alligatoroidea. *Journal of Vertebrate Paleontology*, **19**, 9–100.

—— 2003. Phylogenetic approaches toward crocodylian history. *Annual Review of Earth & Planetary Sciences*, **31**, 357–397.

—— 2010. A new alligatoroid from the Lower Eocene Green River Formation of Wyoming and the origin of caimans. *Journal of Vertebrate Paleontology*, **30**, 1109–1126.

—— 2011. Phylogenetic relationships of *Necrosuchus ionensis* Simpson, 1937 and the early history of caimanines. *Zoological Journal of the Linnean Society*, **163**, S228–S256.

CERDEÑO, E., LÓPEZ, G. M. and REGUERO, M. A. 2008. Biostratigraphic considerations of the Divisaderan faunal assemblage. *Journal of Vertebrate Paleontology*, **28**, 574–577.

CIDADE, G. M. and HSIOU, A. S. 2018. New morphological, evolutionary and paleoecological interpretations on the genus *Eocaiman* (Crocodylia, Caimaninae) from the Cenozoic of South America. 46. *In* MARZOLA, M., MATEUS, O. and MORENO-AZANZA, M. (eds) *Abstract book of the XVI annual meeting of the European Association of Vertebrate Palaeontology*. Universidade Nova de Lisboa, Caparica.

—— SOLÓRZANO, A., RINCÓN, A. D., RIFF, D. and HSIOU, A. S. 2017. A new *Mourasuchus* (Alligatoroidea, Caimaninae) from the late Miocene of Venezuela, the phylogeny of Caimaninae and considerations on the feeding habits of *Mourasuchus*. *PeerJ*, **5**, e3056.

—— RIFF, D., SOUZA-FILHO, J. P. and HSIOU, A. S. 2019*a*. A reassessment of the osteology of *Mourasuchus amazonensis* Price, 1964 with comments on the taxonomy of the species. *Palaeontologia Electronica*, **22**, 1–23.

—— FORTIER, D. and HSIOU, A. S. 2019*b*. The crocodylomorph fauna of the Cenozoic of South America and its evolutionary history: a review. *Journal of South American Earth Sciences*, **90**, 392–411.

—— RIFF, D. and HSIOU, A. S. 2019*c*. The feeding habits of the strange crocodylian *Mourasuchus* (Alligatoroidea, Caimaninae): a review, new hypotheses and perspectives. *Revista Brasileira de Paleontologia*, **22**, 106–119.

—— FORTIER, D. and HSIOU, A. S. 2020*a*. Taxonomic and phylogenetic review of *Necrosuchus ionensis* (Alligatoroidea: Caimaninae) and the early evolution and radiation of caimanines. *Zoological Journal of the Linnean Society*, 189, 657–669.

—— SOLÓRZANO, A., RINCÓN, A. D., RIFF, D. and HSIOU, A. S. 2020*b*. Redescription of the holotype of the Miocene crocodylian *Mourasuchus arendsi* (Alligatoroidea, Caimaninae) and perspectives on the taxonomy of the species. *Historical Biology*, 32, 733–749.

CIFELLI, R. L. 1985. Biostratigraphy of the Casamayoran, early Eocene of Patagonia. *American Museum Novitates*, **2820**, 1–26.

COHEN, K. M., FINNEY, S. C., GIBBARD, P. L. and FAN, J. X. 2013; updated. The ICS International Chronostratigraphic chart. *Episodes*, **36**, 199–204.

COSSETTE, A. P. 2020. A new species of *Bottosaurus* (Alligatoroidea: Caimaninae) from the Black Peaks Formation (Palaeocene) of Texas indicates an early radiation of North American caimanines. *Zoological Journal of the Linnean Society*, zlz178. https://doi.org/10.1093/zoolinnean/zlz178

—— and BROCHU, C. A. 2018. A new specimen of the alligatoroid *Bottosaurus harlani* and the early history of character evolution in alligatorids. *Journal of Vertebrate Paleontology*, **38**, **e1486321**.

ESTABROOK, G. F. 1992. Evaluating undirected positional congruence of individual taxa between two estimates of the phylogenetic tree for a group of taxa. *Systematic Biology*, **41**, 172–177.

FARLOW, J. O., HURLBURT, G. R., ELSEY, R. M., BRITTON, A. R. and LANGSTON, W. 2005. Femoral dimensions and body size of *Alligator mississippiensis*: estimating the size of extinct mesoeucrocodylians. *Journal of Vertebrate Paleontology*, **25**, 354–369.

FARRIS, J. S., KLUGE, A. G. and MICKEVICH, M. F. 1982. Immunological distance and the phylogenetic relationships of the *Rana boylii* species group. *Systematic Zoology*, **31**, 479–491.

FLYNN, J. J. and SWISHER, C. C. 1995. Cenozoic South American land mammal ages: correlation to global geochronologies. 317–333. *In* BERGGREN, W. A., KENT, D. V., AUBRY, M.-P. and HARDENBOL, J. (eds) *Geochronology, time scales, and global stratigraphic correlation*. Society for Sedimentary Geology Special Publication, **54**.

FORTIER, D. C. and RINCÓN, A. D. 2013. Pleistocene crocodylians from Venezuela, and the description of a new species of Caiman. *Quaternary International*, **305**, 141–148.

—— SOUZA-FILHO, J. P., GUILHERME, E., MACIENTE, A. A. and SCHULTZ, C. L. 2014. A new specimen of *Caiman brevirostris* (Crocodylia, Alligatoridae) from the Late Miocene of Brazil. *Journal of Vertebrate Paleontology*, **34**, 820–834.

GASPARINI, Z. 1981. Los Crocodylia fosiles de la Argentina. *Ameghiniana*, **18**, 177–205.

—— 1996. Biogeographic evolution of the South American crocodilians. *Münchner Geowissenschaftliche Abhandlungen*, **30**, 159–184.

GMELIN, J. 1789. *Linnei Systema naturae*. G.E. Beer, Leipzig.

GODOY, P. L., BENSON, R. B., BRONZATI, M. and BUTLER, R. J. 2019. The multi-peak adaptive landscape of crocodylomorph body size evolution. *BMC Evolutionary Biology*, **19**, 167.

—— CIDADE, G. M., MONTEFELTRO, F. C., LANGER, M. C. and NORELL, M. A. 2020. Data from: Redescription and phylogenetic affinities of the caimanine *Eocaiman cavernensis* (Crocodylia, Alligatoroidea) from the Eocene of Argentina. *Dryad Digital Repository*. https://doi.org/10.5061/dryad.xsj3tx9bt

GOLOBOFF, P. A. and CATALANO, S. A. 2016. TNT version 1.5, including a full implementation of phylogenetic morphometrics. *Cladistics*, **32**, 221–238.

—— and SZUMIK, C. A. 2015. Identifying unstable taxa: efficient implementation of triplet-based measures of stability, and comparison with Phyutility and RogueNaRok. *Molecular Phylogenetics & Evolution*, **88**, 93–104.

—— FARRIS, J. S. and NIXON, K. C. 2008. TNT, a free program for phylogenetic analysis. *Cladistics*, **24**, 774–786.

GRAY, J. E. 1844. *Catalogue of tortoises, crocodilians, and amphisbaenians in the collection of the British Museum*. British Museum (Natural History), London.

GRIGG, G. and KIRSHNER, D. 2015. *Biology and evolution of crocodylians*. Cornell University Press, Ithaca, NY.

HALL, P. M. and PORTIER, K. M. 1994. Cranial morphometry of New Guinea crocodiles (*Crocodylus novaeguineae*): ontogenetic variation in relative growth of the skull and an assessment of its utility as a predictor of the sex and size of individuals. *Herpetological Monographs*, **8**, 203–225.

HASTINGS, A. K., BLOCH, J. I., JARAMILLO, C. A., RINCON, A. F. and MACFADDEN, B. J. 2013. Systematics and biogeography of crocodylians from the Miocene of Panama. *Journal of Vertebrate Paleontology*, **33**, 239–263.

—— REISSER, M. and SCHEYER, T. M. 2016. Character evolution and the origin of Caimaninae (Crocodylia) in the New World Tropics: new evidence from the Miocene of Panama and Venezuela. *Journal of Paleontology*, **90**, 317–332.

HEATH, T. A., HUELSENBECK, J. P. and STADLER, T. 2014. The fossilized birth–death process for coherent calibration of divergence-time estimates. *Proceedings of the National Academy of Sciences*, **111**, E2957–E2966.

HELED, J. and BOUCKAERT, R. R. 2013. Looking for trees in the forest: summary tree from posterior samples. *BMC Evolutionary Biology*, **13**, 221.

HURLBURT, G. R., HECKERT, A. B. and FARLOW, J. O. 2003. Body mass estimates of phytosaurs (Archosauria: Parasuchidae) from the Petrified Forest Formation (Chinle Group: Revueltian) based on skull and limb bone measurements. *New Mexico Museum of Natural History & Science Bulletin*, **24**, 105–113.

IORDANSKY, N. N. 1973. The skull of the Crocodilia. 201–262. *In* GANS, C. and PARSONS, T. (eds) *Biology of the reptilia. Vol. 4: Morphology D*. Academic Press.

KAY, R. F., MADDEN, R. H., VUCETICH, M. G., CARLINI, A. A., MAZZONI, M. M., RÉ, G. H., HEIZLER, M. and SANDEMAN, H. 1999. Revised geochronology of the Casamayoran South American Land mammal age: climatic and biotic implications. *Proceedings of the National Academy of Sciences*, **96**, 13235–13240.

LANGSTON, W. 1965. *Fossil crocodilians from Colombia and the Cenozoic history of the Crocodilia in South America*. University of California Publications in Geological Sciences, **52**.

—— 2008. Notes on a partial skeleton of *Mourasuchus* (Crocodylia, Nettosuchidae) from the Upper Miocene of Venezuela. *Arquivos do Museu Nacional*, **66**, 125–143.

LEE, M. S. and YATES, A. M. 2018. Tip-dating and homoplasy: reconciling the shallow molecular divergences of modern gharials with their long fossil record. *Proceedings of the Royal Society B*, **285**, 20181071.

LEWIS, P. O. 2001. A likelihood approach to estimating phylogeny from discrete morphological character data. *Systematic Biology*, **50**, 913–925.

LLOYD, G. T., BAPST, D. W., FRIEDMAN, M. and DAVIS, K. E. 2016. Probabilistic divergence time estimation without branch lengths: dating the origins of dinosaurs, avian flight and crown birds. *Biology Letters*, **12**, 20160609.

LOPEZ, G. M. 2010. Divisaderan: land mammal age or local fauna? 574–577. *In* MADDEN, R. H., CARLINI, A. A., VUCETICH, M. G. and KAY, R. F. (eds) *The paleontology of Gran Barranca: Evolution and environmental change through the middle Cenozoic of Patagonia*. Cambridge University Press.

MADDEN, R. H. and SCARANO, A. 2010. Notes toward history of vertebrate paleontology at Gran Barranca. 46–58. *In* MADDEN, R. H., CARLINI, A. A., VUCETICH, M. G. and KAY, R. F. (eds) *The paleontology of Gran Barranca: Evolution and environmental change through the middle Cenozoic of Patagonia*. Cambridge University Press.

MADDISON, W. P. and MADDISON, D. R. 2018. Mesquite: a modular system for evolutionary analysis. Version 3.51. http://www.mesquiteproject.org

MATEUS, O., PUÉRTOLAS-PASCUAL, E. and CALLAPEZ, P. M. 2019. A new eusuchian crocodylomorph from the Cenomanian (Late Cretaceous) of Portugal reveals novel implications on the origin of Crocodylia. *Zoological Journal of the Linnean Society*, **186**, 501–528.

MATZKE, N. J. and WRIGHT, A. 2016. Inferring node dates from tip dates in fossil Canidae: the importance of tree priors. *Biology Letters*, **12**, 20160328.

NORELL, M. A. 1988. Cladistic approaches to paleobiology as applied to the phylogeny of alligatorids. Unpublished PhD thesis, Yale University, New Haven, CT.

O'REILLY, J. E. and DONOGHUE, P. C. 2017. The efficacy of consensus tree methods for summarizing phylogenetic relationships from a posterior sample of trees estimated from morphological data. *Systematic Biology*, **67**, 354–362.

OAKS, J. R. 2011. A time-calibrated species tree of Crocodylia reveals a recent radiation of the true crocodiles. *Evolution*, **65**, 3285–3297.

ŐSI, A. 2014. The evolution of jaw mechanism and dental function in heterodont crocodyliforms. *Historical Biology*, **26**, 279–414.

—— and BARRETT, P. M. 2011. Dental wear and oral food processing in Caiman latirostris: analogue for fossil crocodylians with crushing teeth. *Neues Jahrbuch für Geologie und Paläontologie-Abhandlungen*, **261**, 201–207.

PAN, T., MIAO, J. S., ZHANG, H. B., YAN, P., LEE, P. S., JIANG, X. Y., OUYANG, J. H., DENG, Y. P., ZHANG, B. W. and WU, X. B. 2020. Near-complete phylogeny of extant Crocodylia (Reptilia) using mitogenome-based data. *Zoological Journal of the Linnean Society*, zlaa074. https://doi.org/10.1093/zoolinnean/zlaa074

PINHEIRO, A. E., FORTIER, D. C., POL, D., CAMPOS, D. A. and BERGQVIST, L. P. 2013. A new *Eocaiman* (Alligatoridae, Crocodylia) from the Itaboraí Basin, Paleogene of Rio de Janeiro, Brazil. *Historical Biology*, **25**, 327–337.

PLATT, S. G., RAINWATER, T. R., THORBJARNARSON, J. B., FINGER, A. G., ANDERSON, T. A. and McMURRY, S. T. 2009. Size estimation, morphometrics, sex ratio, sexual size dimorphism, and biomass of Morelet's crocodile in northern Belize. *Caribbean Journal of Science*, **45**, 80–93.

—— —— —— and MARTIN D. 2011. Size estimation, morphometrics, sex ratio, sexual size dimorphism, and biomass of *Crocodylus acutus* in the coastal zone of Belize. *Salamandra*, **47**, 179–192.

POL, D. and ESCAPA, I. H. 2009. Unstable taxa in cladistic analysis: identification and the assessment of relevant characters. *Cladistics*, **25**, 515–527.

PRICE, L. I. 1964. Sobre o crânio de um grande crocodilídeo extinto do Alto de Rio Juruá, Estado do Acre. *Anais da Academia Brasileira de Ciências*, **56**, 59–66.

R CORE TEAM 2019. *R: A language and environment for statistical computing. v. 3.6.1*. R Foundation for Statistical Computing, Vienna, Austria. https://www.R-project.org/

RAMBAUT, A., DRUMMOND, A. J., XIE, D., BAELE, G. and SUCHARD, M. A. 2018. Posterior summarization in Bayesian phylogenetics using Tracer 1.7. *Systematic Biology*, **67**, 901–904.

RÉ, G. H., BELLOSI, E. S., HEIZLER, M., VILAS, J. F., MADDEN, R. H., CARLINI, A. A., KAY, R. F. and VUCETICH, M. G. 2010. A geochronology for the Sarmiento formation at Gran Barranca. 46–58. *In* MADDEN, R. H., CARLINI, A. A., VUCETICH, M. G. and KAY, R. F. (eds) *The paleontology of Gran Barranca: Evolution and environmental change through the middle Cenozoic of Patagonia*. Cambridge University Press.

RONQUIST, F., KLOPFSTEIN, S., VILHELMSEN, L., SCHULMEISTER, S., MURRAY, D. L. and RASNITSYN, A. P. 2012*a*. A total-evidence approach to dating with fossils, applied to the early radiation of the Hymenoptera. *Systematic Biology*, **61**, 973–999.

—— TESLENKO, M., VAN DER MARK, P., AYRES, D. L., DARLING, A., HÖHNA, S., LARGET, B., LIU, L., SUCHARD, M. A. and HUELSENBECK, J. P. 2012*b*. MrBayes 3.2: efficient Bayesian phylogenetic inference and model choice across a large model space. *Systematic Biology*, **61**, 539–542.

SALAS-GISMONDI, R., FLYNN, J. J., BABY, P., TEJADA-LARA, J. V., WESSELINGH, F. P. and ANTOINE, P. O. 2015. A Miocene hyperdiverse crocodylian community reveals peculiar trophic dynamics in proto-Amazonian mega-wetlands. *Proceedings of the Royal Society B*, **282**, 20142490.

SANAIOTTI, T., MAGNUSSON, W. and CAMPOS, Z. 2010. Maximum size of dwarf caiman, *Paleosuchus palpebrosus* (Cuvier, 1807), in the Amazon and habitats surrounding the Pantanal, Brazil. *Amphibia-Reptilia*, **31**, 439–442.

SCHEYER, T. M., AGUILERA, O. A., DELFINO, M., FORTIER, D. C., CARLINI, A. A., SÁNCHEZ, R., CARRILLO-BRICEÑO, J. D., QUIROZ, L. and SÁNCHEZ-VILLAGRA, M. R. 2013. Crocodylian diversity peak and extinction in the late Cenozoic of the northern Neotropics. *Nature Communications*, **4**, 1907.

—— HUTCHINSON, J. R., STRAUSS, O., DELFINO, M., CARRILLO-BRICEÑO, J. D., SANCHEZ, R. and SANCHEZ-VILLAGRA, M. R. 2019. Giant extinct caiman breaks constraint on the axial skeleton of extant crocodylians. *eLife*, **8**, e49972.

SERENO, P. C., LARSSON, H. C., SIDOR, C. A. and GADO, B. 2001. The giant crocodyliform *Sarcosuchus* from the Cretaceous of Africa. *Science*, **294**, 1516–1519.

SIMPSON, G. G. 1930*a*. Scarritt-Patagonian Exped. Field Notes (Book 1). American Museum of Natural History (unpublished), New York. http://research.amnh.org/paleontology/notebooks/simpson-1930a/

—— 1930*b*. Scarritt-Patagonian Exped. Field Notes (Book 2). American Museum of Natural History (unpublished), New York. http://research.amnh.org/paleontology/notebooks/simpson-1930b/

—— 1933*a*. A new crocodilian from the *Notostylops* Beds of Patagonia. *American Museum Novitates*, **623**, 1–9.

—— 1933*b*. A new fossil snake from the *Notostylops* Beds of Patagonia. *Bulletin of the American Museum of Natural History*, **67**, 1–22.

—— 1933*c*. Stratigraphic nomenclature of the early Tertiary of central Patagonia. *American Museum Novitates*, **644**, 1–13.

—— 1934*a*. *Attending marvels: A Patagonian journal*. Time, New York, NY.

—— 1937. An ancient eusuchian crocodile from Patagonia. *American Museum Novitates*, **965**, 1–20.

SOUZA-FILHO, J. P., SOUZA, R. G., HSIOU, A. S., RIFF, D., GUILHERME, E., NEGRI, F. R. and CIDADE, G. M. 2019. A new caimanine (Crocodylia, Alligatoroidea) species from the Solimões Formation of Brazil and the phylogeny of Caimaninae. *Journal of Vertebrate Paleontology*, **38**, e1528450.

SPALLETTI, L. A. and MAZZONI, M. M. 1977. Sedimentología del Grupo Sarmiento en un perfil ubicado al sudeste del Lago Colhué Huapí, provincia de Chubut. *Obra del Centenario del Museo de la Plata*, **4**, 261–283.

—— —— 1979. Estratigrafia de la Formación Sarmiento en la barranca sur del Lago Colhué-Huapí, provincia del Chubut. *Revista de la Asociación Geológica Argentina*, **34**, 271–281.

STADLER, T. 2010. Sampling-through-time in birth-death trees. *Journal of Theoretical Biology*, **267**, 396–404.

THORBJARNARSON, J. 1992. *Crocodiles: An action plan for their conservation*. International Union for Conservation of Nature, Gland, Switzerland, 136 pp.

VERDADE, L. M. 2000. Regression equations between body and head measurements in the broad-snouted caiman (*Caiman latirostris*). *Revista Brasileira de Biologia*, **60**, 469–482.

WEBB, G. J. W. and MESSEL, H. 1978. Morphometric analysis of *Crocodylus porosus* from the north coast of Arnhem Land, northern Australia. *Australian Journal of Zoology*, **26**, 1–27.

WHITING, E. T., STEADMAN, D. W. and VLIET, K. A. 2016. Cranial polymorphism and systematics of Miocene and living *Alligator* in North America. *Journal of Herpetology*, **50**, 306–315.

ZHANG, C., STADLER, T., KLOPFSTEIN, S., HEATH, T. A. and RONQUIST, F. 2016. Total-evidence dating under the fossilized birth-death process. *Systematic Biology*, **65**, 228–249.